Depth migration of deep seismic reflection profiles: crustal thickness variations in Alberta

Youcef Bouzidi, Douglas R. Schmitt, Ronald A. Burwash, and Ernest R. Kanasewich

Abstract: Variations in crustal thickness provide important clues as to the formation of the crust, present-day isostatic equilibrium, and crustal stress. The map of the topography of the Mohorovicic discontinuity in Alberta is revised using 1900 km of reanalysed seismic reflection profiles acquired as part of the Lithoprobe Alberta Basement Transect. Time sections were depth migrated using a parallelized algorithm that accounts for steeply dipping structures. The migration process employed a geologically consistent velocity model of the metamorphic crust derived from earlier refraction experiments and constrained by compilations of high-pressure rock velocity measurements. We found that knowledge of the velocities in the sedimentary column strongly influenced the quality of the migration calculations. The Mohorovičić discontinuity is generally distinguished in these profiles, on the basis of sharp changes in reflectivity, at depths of 35–48 km. Sharp reflections from this boundary are rare. A number of geologic features are of note in these lines. A localized (~50 km extent) crustal thinning is observed in the Peace River region; this thinning is consistent with an adjacent oxygen isotopic anomaly indicative of crustal extension. In central Alberta, the Mohorovičić discontinuity topography is suggestive of a sharp jump of 10 km indicative of mantle faulting associated with the Snowbird tectonic zone. In southern Alberta, the crust thickens substantially across the Vulcan structure, with the greatest thickness correlating with the Vulcan structure itself indicating a collisional origin as noted by other authors.

Résumé : Des variations dans l'épaisseur de la croûte fournissent d'importants indices quant à la formation de la croûte, au présent équilibre isostatique et aux contraintes dans la croûte. La carte de la topographie de la discontinuité de Mohorovicic en Alberta est révisée en utilisant 1900 km de profils réanalysés de sismique réflexion acquis du transect Lithoprobe du socle de l'Alberta. Des sections de temps ont été migrées vers le bas en utilisant un algorithme de mise en parallèle qui tient compte des structures à fort pendage. Le processus de migration utilise un modèle de vitesse qui concorde géologiquement avec la croûte métamorphique, dérivé d'essais antérieurs de réfraction et limité par des compilations de mesures de vitesse dans les roches à haute pression. Nous avons trouvé que la connaissance des vitesses dans la colonne sédimentaire influence grandement la qualité des calculs de migration. La discontinuité de Mohorovicic se distingue habituellement dans ces profils, sur la base de changements abrupts dans la réflectivité, à des profondeurs de 35 à 48 km. Des réflexions bien définies de cette limite sont rares. Certaines caractéristiques géologiques sont dignes de mention dans ces lignes. Un amincissement localisé de la croûte (d'une étendue ~50 km) est observé dans la région de Peace River; cet amincissement concorde avec une anomalie voisine en oxygène isotopique indiquant une extension de la croûte. Au centre de l'Alberta, la topographie de la discontinuité de Mohorovicic suggère un saut abrupt de 10 km indiquant des failles dans la croûte associées à la zone tectonique Snowbird. Au sud de l'Alberta, la croûte s'épaissit considérablement en travers de la structure de Vulcan et le plus grand épaississement correspond à la structure de Vulcan, elle-même indiquant une origine de collision telle que notée par d'autres auteurs.

[Traduit par la Rédaction]

Introduction

Knowledge of the crustal thickness is fundamentally important to a number of issues in the earth sciences. Isostasy links, in part, crustal thickness to surface topography; improved knowledge of crustal thickness variations allows for better understanding of isostatic rebound and for more subtle detection of variations in density of upper mantle material. Because of temperature-dependent rheology, the uppermost crust bears much of the lithospheric stress load and crustal thickness variations, in conjunction with other information such as geothermal gradients, are necessary to the general interpretation of crustal stress observations. Finally, regional and teleseismic arrivals must pass through much of the crust

Received 7 March 2001. Accepted 1 October 2001. Published on the NRC Research Press Web site at http://cjes.nrc.ca on 29 March 2002.

Paper handled by Associate Editor F. Cook.

Y. Bouzidi[1], D.R. Schmitt, R.A. Burwash[2], and E.R. Kanasewich[3]. Department of Physics, University of Alberta, Edmonton, AB T6G 2J1, Canada.
[2]Also Department of Earth and Atmospheric Sciences, University of Alberta, Edmonton, AB T6G 2E3, Canada.
[3]Deceased.

 DOI: 10.1139/E01-080

on their way to a detector, and the capability to properly correct for this variation can improve the reliability of global scale tomographic inversions and earthquake source location.

These requirements have stimulated numerous studies employing a variety of methods aimed at estimating variations in crustal thickness and velocity structure as reviewed by Tanimoto (1995). Based on wide-angle refraction experiments and surface wave dispersion, a number of continental-scale crustal thickness maps have been compiled for North America (Braile et al. 1989), Europe (Meissner 1986), and the whole earth (Soller et al. 1982; Mooney et al. 1998; Christensen and Mooney 1995; Nataf and Ricard 1996).

The above studies provide regional averages of crustal structure. However, crustal thicknesses vary over lateral dimensions of 100 km or less and these more local variations can provide important clues to crustal formation. Thinner crust is expected in areas that have undergone extension, such as the present-day Basin and Range province. Thicker crust is to be found in collisional zones, such as the Himalayas, where continental material of the Indian subplate is being subducted beneath Asia. Sharp changes in crustal thickness can indicate thrust faulting across the Mohorovičić discontinuity (e.g., Zhu 2000).

Wide-angle seismic refraction experiments provide good estimates of crustal thickness and velocity variations. Great progress has been made in the acquisition and analysis of such profiles; for example, many hundreds of detectors are employed in modern surveys, and inversions account not only for traveltimes but also incorporate amplitudes and waveform character to better delineate structure. However, the lateral resolution available by such techniques remains limited by the very nature of the refraction experiment.

In contrast, deep seismic reflection profiles highlight small lateral structural variations in terms of traveltime and surface position but cannot further delineate the structure in terms of its seismic velocity. A second problem with deep seismic reflection profiling is that positioning errors of dipping features can be substantial, and diffractions can interfere with desired reflections. In seismology, migration refers to the process of correcting the raw reflection profile for both incorrectly positioned and unfocussed seismic events. Of the plethora of migration methodologies, depth migration is the most sophisticated allowing one to account for lateral variations in the structure. An added bonus of depth migration algorithms is that they can reproduce the seismic profile in both time and depth within the earth.

The structure of the metamorphic crust is complex, and consequently, even crustal-scale profiles will benefit from migration. In this paper, the depth migration of over 1900 km of seismic reflection profiles obtained for the Lithoprobe Alberta Basement Transect is carried out using a geologically consistent velocity model constrained by refraction results. Since, to our knowledge depth migration has not been employed previously in crustal imaging, some of the technical aspects and problems involved with such large data sets are described, especially those resulting from the existence of an overlying thick sedimentary sequence. A revised map of crustal thickness in central and southern Alberta is provided from the integration of previous refraction results (Dufresne et al. 1996) with the present depth-migrated sections. These new estimates of crustal depth along the profiles are then discussed in the context of three different geologic features of the Proterozoic metamorphic crust in Alberta.

Lithoprobe reflection surveys

A number of refraction and reflection studies served as motivations for Lithoprobe studies in Alberta beginning as early as 1959 (Richards and Walker 1959; Weaver 1963; Maureau 1965; Chandra 1966; Kanasewich 1966; Cumming and Kanasewich 1966; Kanasewich et al. 1969; Chandra and Cumming 1972; Ganley and Cumming 1974; Mereu et al. 1977; Zelt and Ellis 1989*a*, 1989*b*; Stephenson et al. 1989; and Halchuk and Mereu 1990). As well, much pioneering work on deep crustal and Mohorovičić discontinuity reflections was carried out in Alberta (Kanasewich and Cumming 1965; Cumming and Kanasewich 1966; Clowes et al. 1968; Clowes and Kanasewich 1972; Ganley and Cumming 1974; Zelt and Ellis 1989*a*).

Three deep seismic reflection experiments were acquired in Alberta for the Lithoprobe Alberta Basement Transect. The Central Alberta Transect (CAT, lines 1 through 10) consists of 521 km of profiles recorded over central Alberta in 1991. The profiles extend from about 100 km west of Edmonton to the Saskatchewan border (Figs. 1–3). The intention of these profiles was to study the Rimbey, Wabamun, and Thorsby domains (see Ross et al. (1991) and Villeneuve et al. (1993) for a description of the various domains) associated with the Snowbird tectonic zone and also the Eyehill magnetic high at the Saskatchewan border (Fig. 2). Nearly 608 km of profiles (lines 11a to 20b) were obtained in the second segment in 1994 in the north-western Alberta by a consortium for the Peace River Arch Industrial Seismic Experiment (PRAISE). This series was expected to provide further insight on the regional tectonic evolution of the crust over the enigmatic Peace River Arch. These profiles crossed the Ksituan, Chinchaga, and Buffalo Head tectonic domains (Ross et al. 1991;Villeneuve et al. 1993). The final 785 km of profiles (lines 21 to 32) was acquired in the Southern Alberta Lithospheric Transect (SALT) program in 1995. The Vulcan Low was one significant target of this survey.

The acquisition parameters and processing stream are summarized in Table 1. More specific details are found in Kanasewich et al. (1993) for the CAT surveys, Eaton and Ross (1996) for SALT surveys, and Eaton (1995) for the PRAISE surveys.

Depth migration procedures

The stacked Lithoprobe reflection profiles of the Alberta Basement Transect exhibit many diffraction patterns and steeply dipping events. Many cross-dipping events are present in the unmigrated sections, and this substantially complicates their interpretation (example given in Fig. 4*a*); migration is necessary to allow for less ambiguous geologic interpretations. The migrated section (Fig. 4*b*) often differs substantially from the unmigrated section (Fig. 4*a*). In particular the misplaced dipping event in Fig. 4*a* is shortened substantially and moved upward to the left about 12 km laterally from its initial position. The original commercial processing incorporated an economic time migration based on a modified finite difference algorithm. While the resulting profiles are an

Fig. 1. Locations and numbering of Lithoprobe Alberta Basement reflection surveys. Magnetically defined tectonic domains of Villeneuve et al. (1993) are indicated: GB, Great Bear; Ht, Hottah; Nv, Nova; Ks, Ksituan; Ch, Chinchaga; BH, Buffalo Head; Tl, Taltson; Wb, Wabamun; Th, Thorsby; Rm, Rimbey; Lc, Lacombe; Lo, Loverna; Eh, Eyehill; Vl, Vulcan; MH, Medicine Hat. Locations of mantle topographic features discussed later text include the Spirit River mantle high, the Edmonton mantle low within the Snowbird tectonic zone, and the Vulcan mantle low. CAT, Central Alberta Transect; PRAISE, Peace River Arch Industrial Seismic Experiment; SALT, Southern Alberta Lithospheric Transect.

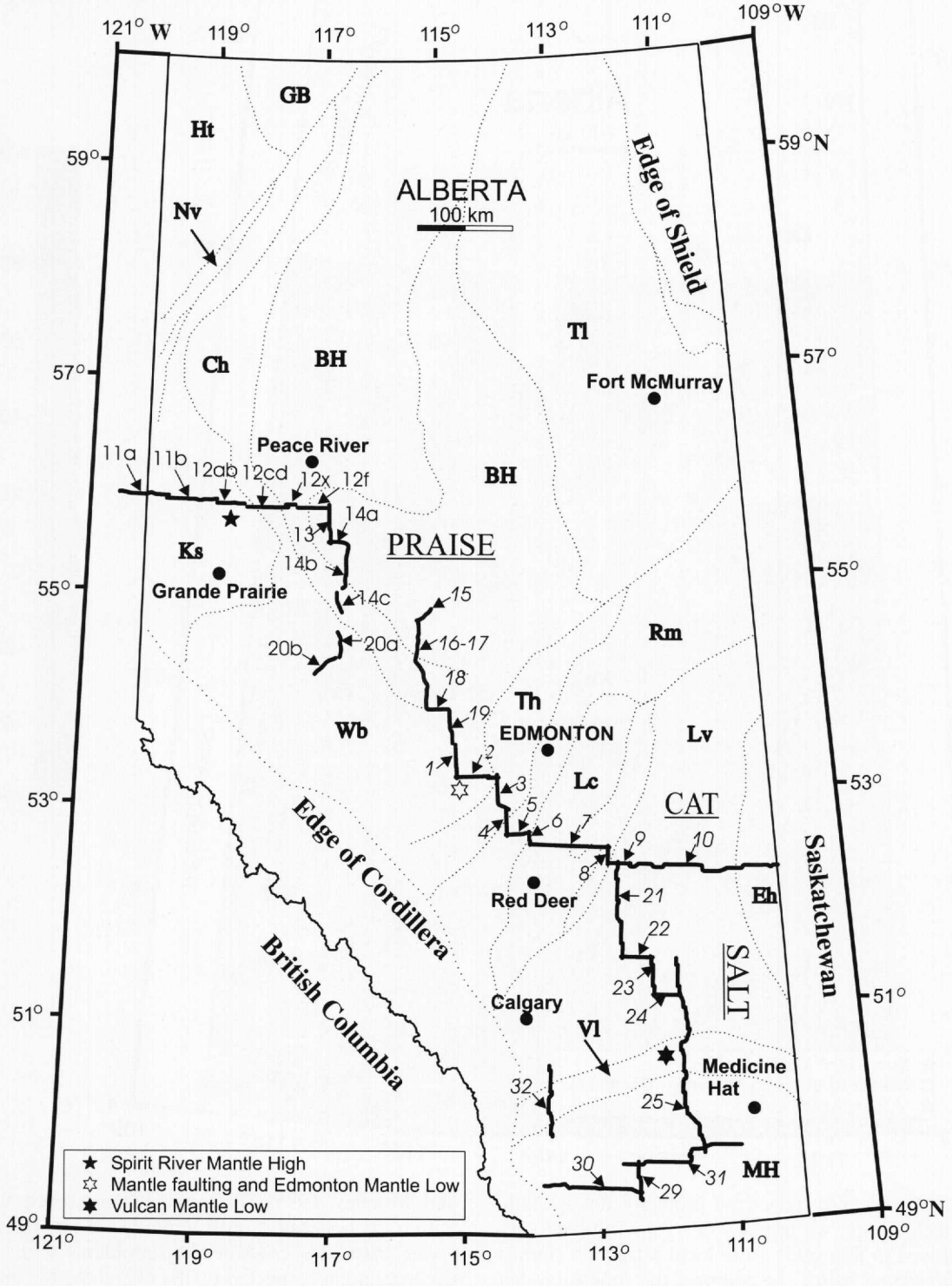

improvement over the unmigrated profiles, determination of the depth of features within the crust can still be problematic. Comparisons of the quality of seismic images produced by either conventional time or the present depth migration is highly subjective. The value of the present depth migration lies, however, in the fact that the depth migration accommodates as input the interval velocity structure with lateral variations. While we cannot claim that an absolutely correct velocity

Fig. 2. Locations of Lithoprobe Alberta Basement reflection surveys and magnetically defined tectonic regimes of Villeneuve et al. (1993) superimposed on background of magnetic field intensity. Refer to Fig. 1 for seismic profile index. Domain abbreviations as in Fig. 1.

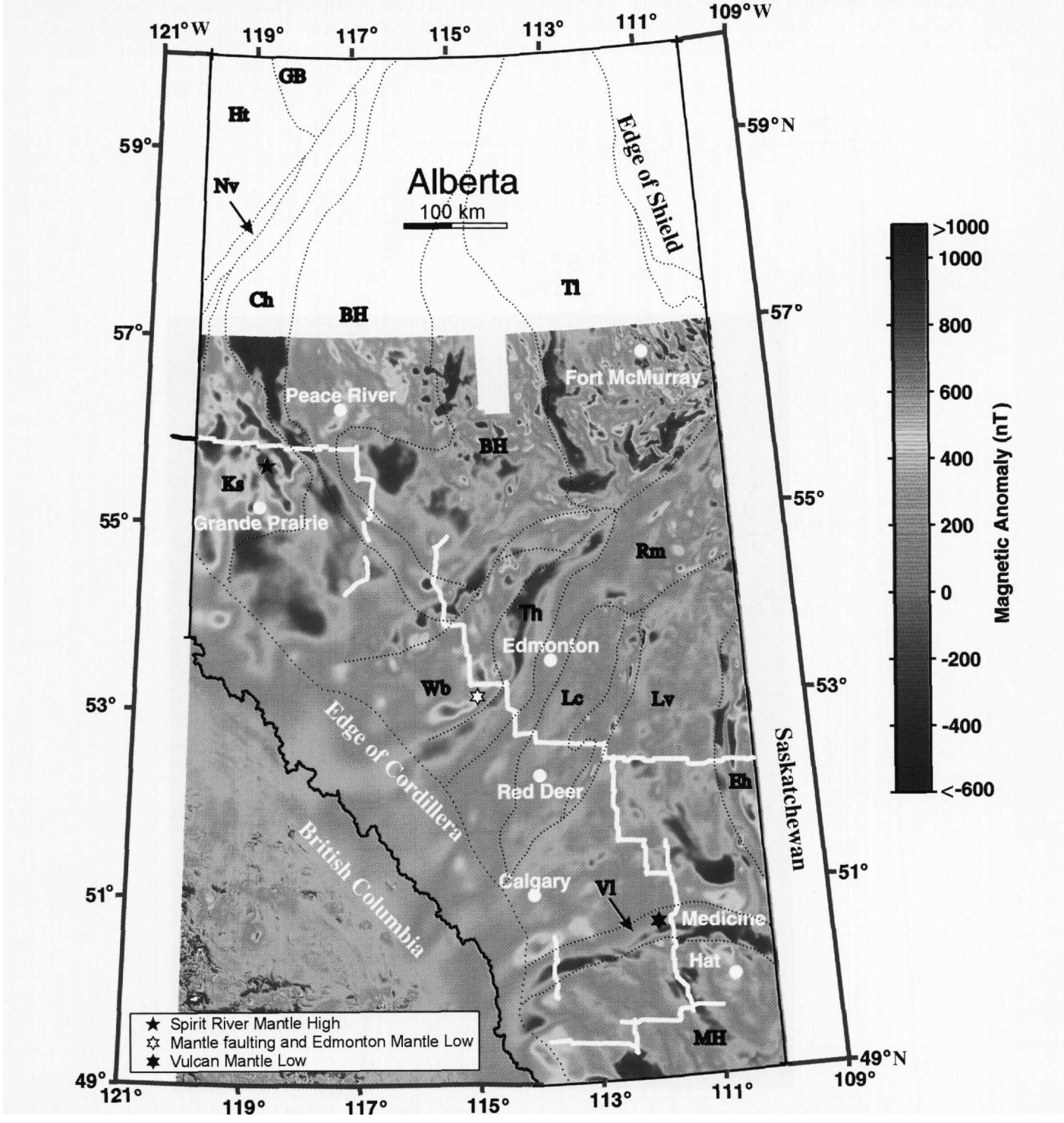

function is employed and, indeed, is probably unknowable with current technology, we initially developed the velocity function employed in this study from local refraction studies with details presented below. In contrast, the time migrated profiles employed a simple constant velocity of 6.7 km/s below 6 s and 8.3 km/s within the upper most mantle, a value that reflects an expected average of expected compressional wave velocities through the crust (Christensen and Mooney 1995). This value can exceed the velocities within the uppermost crust while being less than those in the lower crust; this could lead to problems with over and under-migration, respectively. To overcome the problem of accurate depth estimation in this study, the stacked raw profiles were depth migrated using a more realistic velocity model.

Many of the geologic features that produce reflections in

Fig. 3. Locations of Lithoprobe Alberta Basement reflection surveys superimposed on background of Bouguer gravity. Refer to Fig. 1 for seismic profile index. FdL delineates the Fond du Lac paired gravity high–low (Burwash and Muehlenbachs 1997).

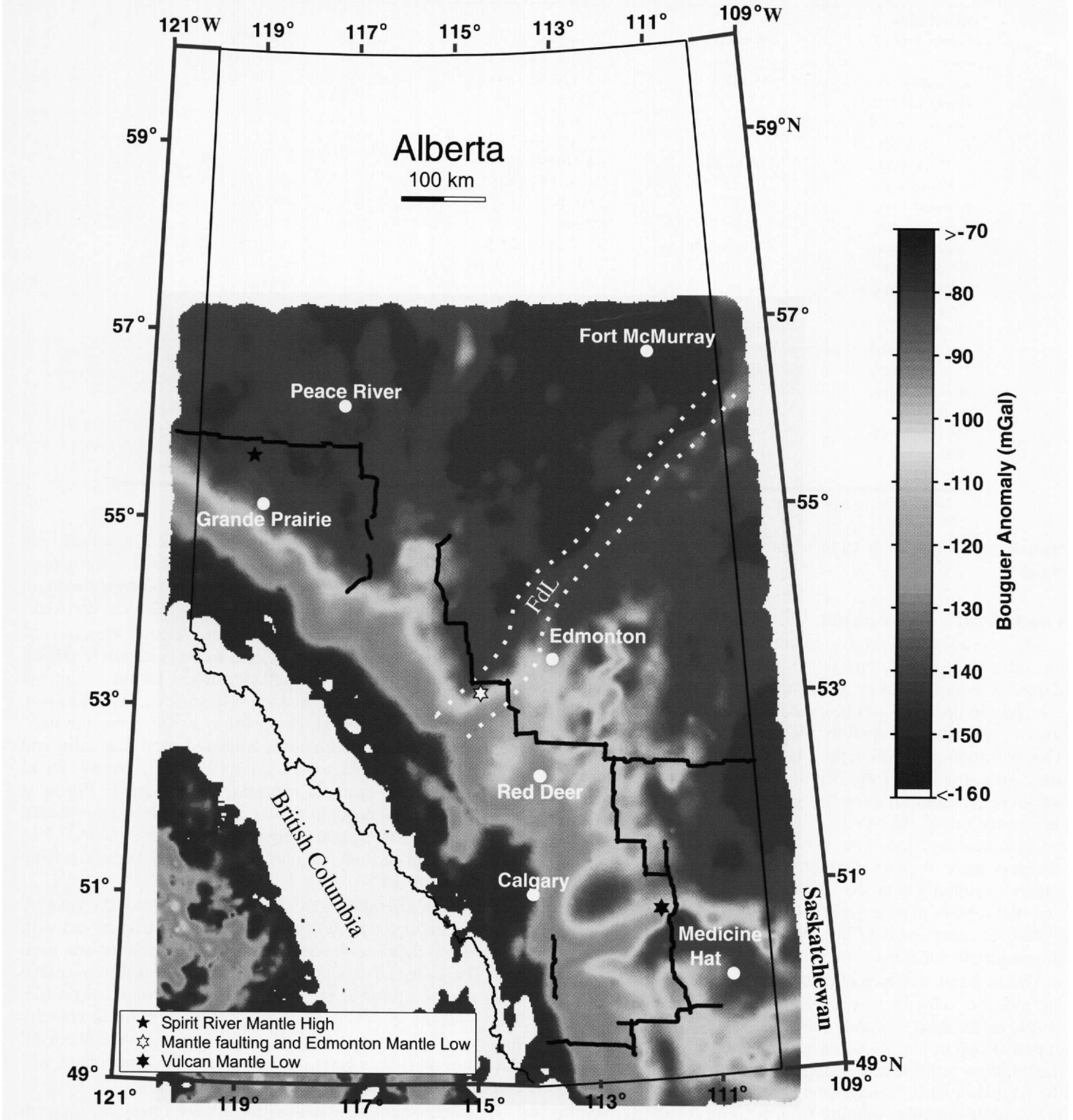

the profiles have a substantial dip (>45°), and more sophisticated migration algorithms are necessary to avoid spatial aliasing of steeply dipping events by the migration process (see Yilmaz 1987 for a discussion of these issues). A specialized in-house depth migration routine developed by S. Phadke and E.R. Kanasewich was employed. Briefly, the algorithm is an adaptation of a conventional finite difference depth migration in the ω-x domain (Claerbout 1985; Yilmaz 1987) employing a new set of expansion coefficients determined using a least squares minimisation (Bunks 1992). This algorithm can handle dips to 70° but at a computational cost equal to that of standard 45° routines. To achieve further reductions in computation time and allow for the iterative migrations described below, the process was implemented in a parallel virtual machine environment. Despite these economies, the larger sections (~8000 common-midpoint stacked traces) re-

Table 1. Summary of acquisition parameters and processing stream for the Lithoprobe Alberta Basement Transects.

	CAT	PRAISE	SALT
Acquisition			
Source type	Vibroseis	Vibroseis	Vibroseis
Sweep	10–56 Hz; 14 s	10–80 Hz; 14 s	10–80 Hz; 20 s
Recording filter	3–90 Hz	3–120 Hz	3–120 Hz
Group interval	50 m	25 m	25 m
Source interval	100 m	100 m	100 m
Recording spread			
Trace number	1 60 61 240	1 240 241 480	1 240 241 480
Distance (m)	3100 150 150 9100	6050 75 75 6050	6050 75 75 6050
Nominal fold	6000%	6000%	6000%
Sampling rate	4 ms	2 ms	2 ms
Source pattern	4 vibroseis/50 m	4 vibroseis/25 m	4 vibroseis/25 m
Record length	18 s (final)	Alternating 20 and 32 s	32 s
Receiver pattern	9/42 m	9/25 m	9/25 m
Processing			
Geometry	Straight line	Crooked line	Crooked line
Automatic Gain Control	500 ms	500 ms	500 ms
Deconvolution	Designature	Spiking. Operator: 80 ms	Designature
Spectral balance	Multiple gate		Multiple gate
Statics	Refraction + Residual	Floating datum + fixed datum +residual	Refraction + Residual
Deconvolution	F-X		F-X
Scaling	Multiple gate AGC	Trace Balance	Multiple gate AGC
Filtering	Time-variant bandpass		Time-variant bandpass

Note: AGC, automatic gain control.

quired more than 24 h each to process on a 22-node machine.

Constrained velocity model

All migration procedures require a reasonable model of the velocity structure with depth and surface position in the Earth. Standard industry practice assumes that the interval velocities in the Earth can be estimated from the corresponding stacking velocities obtained for the normal move-out correction. This assumption is valid for shallow data when the offsets are a large fraction of the depth of investigation and there is sufficient curvature in move-out curves to allow for reasonable determination of the stacking velocities. However, in deep seismic profiling the time move-out of a deep reflector at 10 km or more of offset from the source in a common midpoint gather essentially vanishes. Consequently, from such data, one may obtain a wide variety of velocities, many of which would not represent the true geologic structure and hence are inappropriate for use in migration.

This problem was overcome in the present survey by adapting the average velocity model compiled by Kanasewich et al. (1994) on the basis of earlier refraction surveys of the Canadian craton. Kopp et al. (2000) have conducted a similar study in the Makran accretionary wedges between the Eurasian and the Arabian plates. Kanasewich et al.'s model consists of five layers with velocities ranging from 5.5 km/s at the surface to 7.1 km/s in the lower crust and compares favourably with the global average model developed by Christensen and Mooney (1995) from both deep seismic refraction studies and thousands of high-pressure laboratory velocity measurements. Kanasewich et al.'s model was modified by calculating linear gradients to provide a final basis velocity function (Fig. 5). This basis function was scaled appropriately to depth as described below and was employed in all the migrations. More complicated lateral heterogeneities in velocity are ignored. However, in the absence of additional information, there is little justification at the present time for employing a more complex model, and Occam's principle was invoked.

In contrast, lateral variations in the velocity structure of the sedimentary column were found to be particularly critical to the depth migration. The velocity model for the sediments was derived directly from stacking velocities via Dix's formula, used to create the initial stack. Prior to this step, however, inconsistent stacking velocities were removed manually and a trace-by-trace velocity function was derived by linear interpolation. An example from line 23 is given in Fig. 6. It was found that the depth to the metamorphic basement predicted by the migration agreed well (generally better than 2.5%) with those known from deep drilling in the sedimentary column (Wright et al. 1994).

The depth migration was employed twice, with the velocity model being updated in the second cycle. A trial model with a presumed depth to the Mohorovičić discontinuity was used first. The estimated depth to the discontinuity was then measured manually at a number of points in the new migrated profile. These picked depths were used to scale the basis velocity function of Fig. 5 on a trace-by-trace basis to the new crustal thickness and the migration was rerun. This procedure was employed for all sections.

It is important to discuss the uncertainties of such an approach. Using the upper and lower bounds of the velocity with depth structure of Christensen and Mooney (1995), as shown in Fig. 5 from below 5 km depth, a depth to the Mohorovičić discontinuity of 45 km gives an uncertainty of about ±2 km. This accounts for the uncertainty due to the sedimentary column as just discussed in addition to those uncertainties due to the spread of velocity with depth shown by the grey area of fig. 5 in Christensen and Mooney (1995).

Figs. 4. Examples of features before and after depth migration of a portion of line 25. The arrows show a dipping (moderate dip) event (*a*) before and (*b*) after migration (semblance enhanced). Note the lateral displacement of this event by the migration process (about 12 km to the left). The migrated section differs substantially from the unmigrated one. The Moho is better defined after migration.

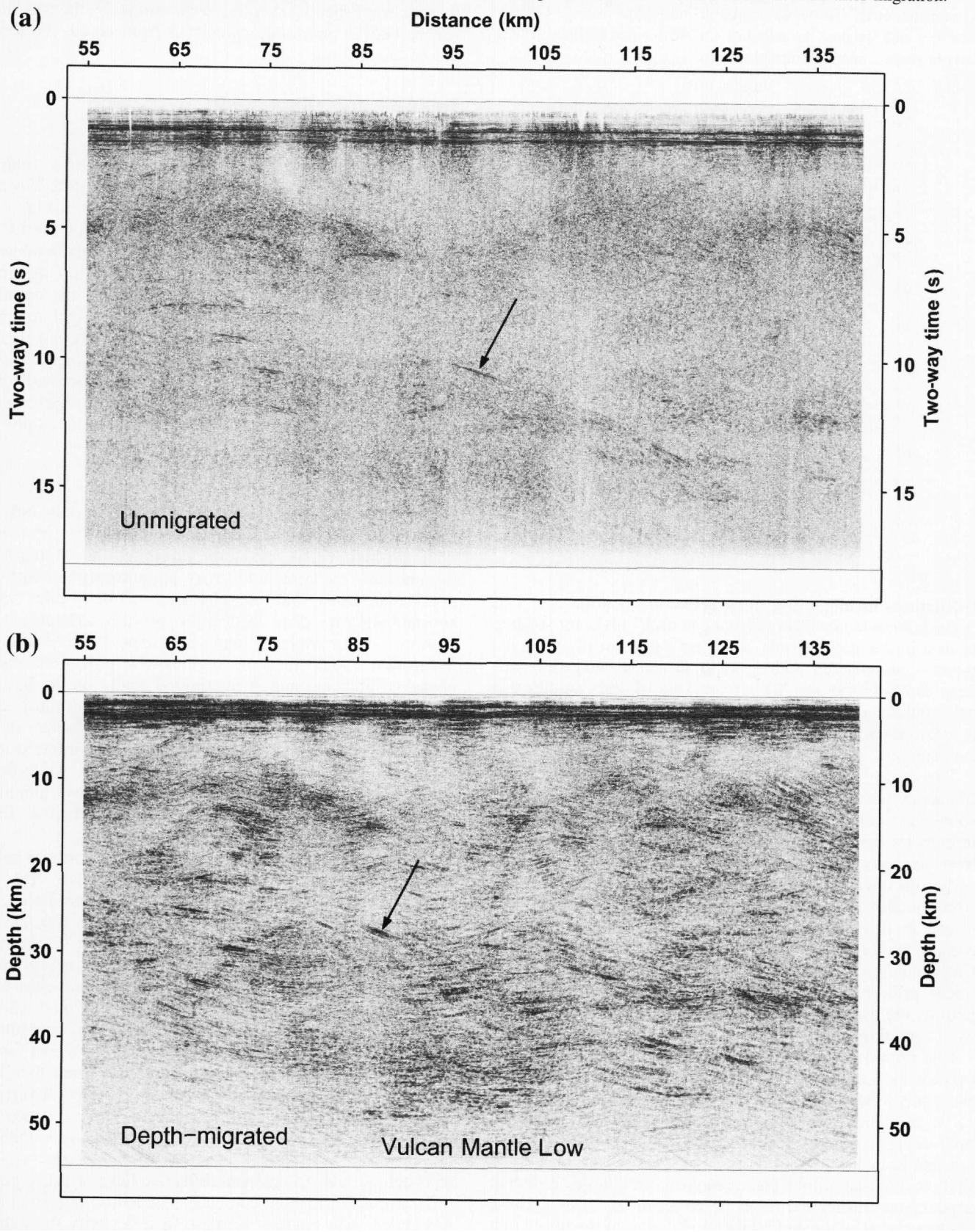

Fig. 5. Model of seismic velocity versus depth employed for crystalline portions of the crust. Black line is the velocity versus depth function extracted from regional seismic refraction measurements compiled by Kanasewich et al. (1994). Grey area delineates the average crustal velocities with standard deviations of Christensen and Mooney (1995) derived from laboratory measurements.

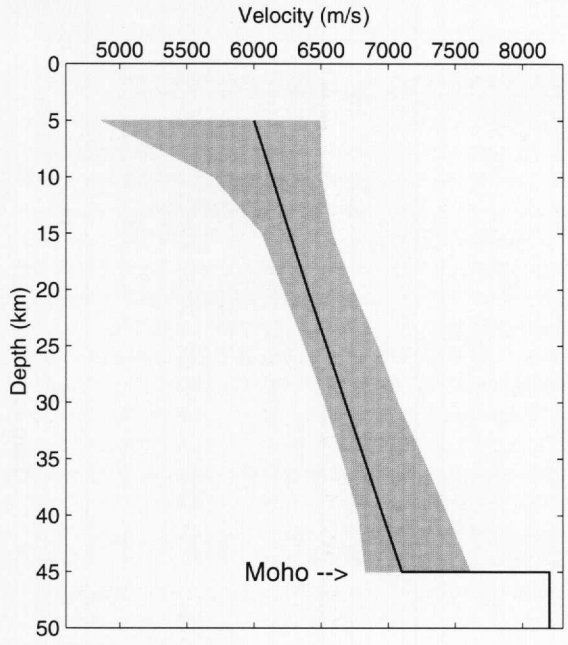

Difficulties in migrating deep reflection profiles

Aside from the problem of having to deal with larger volumes of data in the deep records, there are a number of additional issues that must be addressed to properly carry out such deep depth-migrations. We are unaware of other studies that have employed depth-migration techniques to such data sets; it is important to briefly discuss some of the problems encountered.

The quality of these data varies from line to line. High-frequency noise (>80 Hz), the origin of which is unknown, sometimes dominates the energy spectrum of many lines at long times despite the fact that the vibrator sweeps were at lower frequency. This suggests the noise is an artefact of the earlier deconvolution. Signal components above 50 Hz were strongly attenuated within the sedimentary column, as determined in filter tests which demonstrated that no coherent events could be discerned in the profiles after high-pass filtering. Consequently, a 10–50 Hz band pass filter was applied to the traces prior to depth migration. This frequency limitation permits the use of a coarse depth step of 25 m in the present case, reducing substantially the running time.

It is important to note that most of the energy within the traces is localized at early times within the sedimentary column, especially at less than 1 s of two-way traveltime. These high, early amplitudes caused serious difficulties for the depth migration because of repetitive wrap-around effects in the Fourier domain. In particular, the impulse response of a shallow, high-amplitude spike reappears as a large artefact at depth compromising the resolving power of the section. These artefacts were attenuated by the modulation of the upper first second of the original sections with a cosine taper. This process reduces artefacts in later time in the sections. Trace-to-trace amplitude normalization was further applied to minimize the effect of spurious lateral amplitude variations. This was accomplished by dividing each sample by the root mean square (RMS) amplitude calculated from below the top of the basement only.

Results and discussion

Migrated sections

All of the final migrated sections are provided as foldouts in Fig. 7 with depths given relative to an orthometric elevation of 1 km above sea level. These results shown in Fig. 7 are not the direct output of the migration process but are further processed by the application of a lateral coherency semblance-based filter to enhance continuous events within the crust. Actual picking of depth of the Mohorovičić discontinuity was, however, carried out on the directly output migrated profiles. Depth-dependent amplitude gains were not used to avoid disturbing the sometimes subtle changes in the reflected amplitudes used to detect the reflection Mohorovičić discontinuity. The Mohorovičić discontinuity depths determined from the directly output migrated profiles agree well with those interpreted from Fig. 7.

Crustal thickness variations

An accurate estimate of crustal thickness can only be made if the Mohorovičić discontinuity itself can be readily distinguished. From refraction profiling, the Mohorovičić discontinuity is known to exist ubiquitously beneath the continental crust, but the character of the Moho varies substantially in deep reflection profiles (Hammer and Clowes 1997; Mooney and Meissner 1992; Hale and Thompson 1982). In some regions, the reflection seismic Moho is indistinct and is interpreted solely on the basis of an abrupt change in the reflectivity. That is, over most of the lines, there is a distinct depth-dependent change in the strength of the returned signal. Above what is inferred to be the Moho, numerous short events are returned, while below it, the images display noticeably fewer and lower amplitude events such that this region is often referred to as being "transparent." In the semblance enhanced images of Fig. 7, this behaviour is perhaps best retained in the northern half of line 25, where high-amplitude events dominate from the base of the sedimentary layer to depths of 42 km. Below this depth, the reflectivity is noticeably diminished. The fact that this boundary occurs quickly suggests it must be produced by a first-order change in geology and is hence interpreted to be from the Moho. More rarely, a continuous and clear event may be interpreted as the Moho. Hammer and Clowes (1997) summarized a series of observations of the Moho in the large set of Lithoprobe reflection profiles, which sample crust of a variety of ages and tectonic environments. They provided three classifications consisting, repeated in verbatim here, of class 1, a distinct, narrow (< 0.3 s two-way traveltime), multicyclic band of reflectors that are continuous or piece-wise continuous over tens of kilometres; class 2, well-defined transitions from reflective lower crust to poorly reflective upper mantle; and class 3, a diffuse transition zone associated with gradual decrease in reflectivity through the lower crust. The reasons for this variety in character range

Figs. 7*a*–7*b*. Depth-migrated and coherency-enhanced seismic section across Ksituan, Chinchaga, and Buffalo Head domain

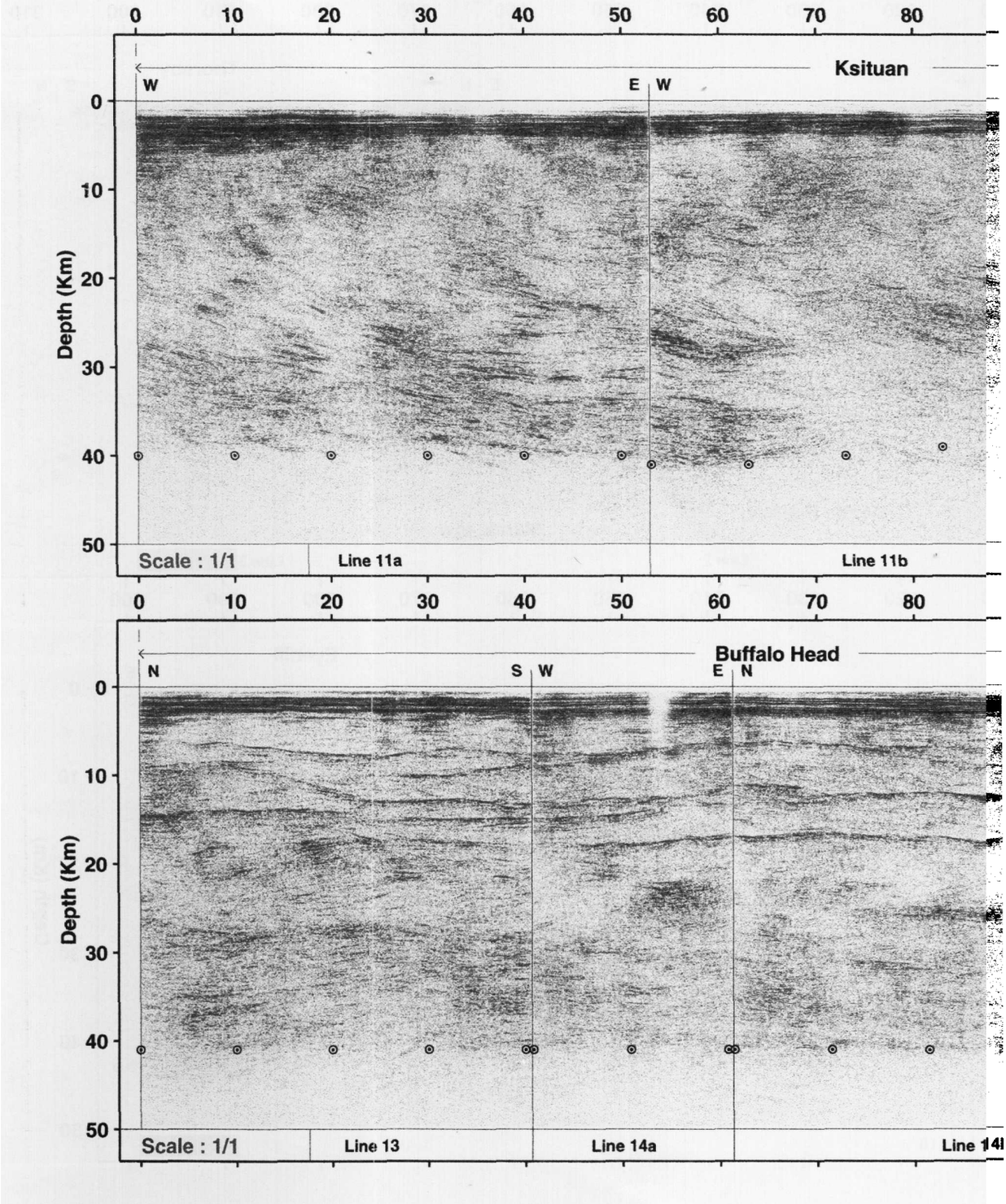

omains.

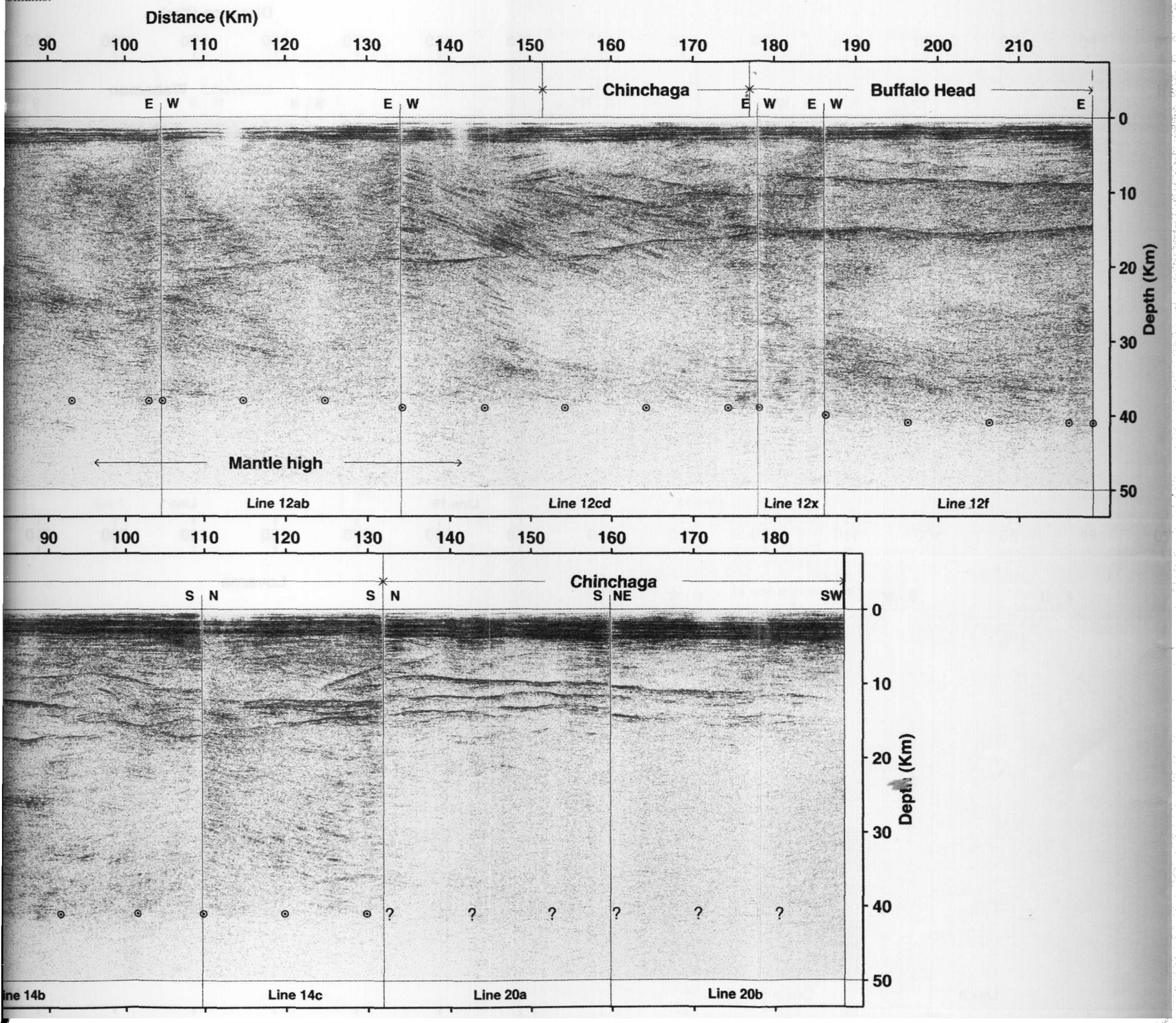

Figs. 7*c*–7*d*. Depth-migrated and coherency-enhanced seismic section across Buffalo Head, Wabamun, Thorsby, Rimbey, Lacombe, Loverna, and Eye Hill domain

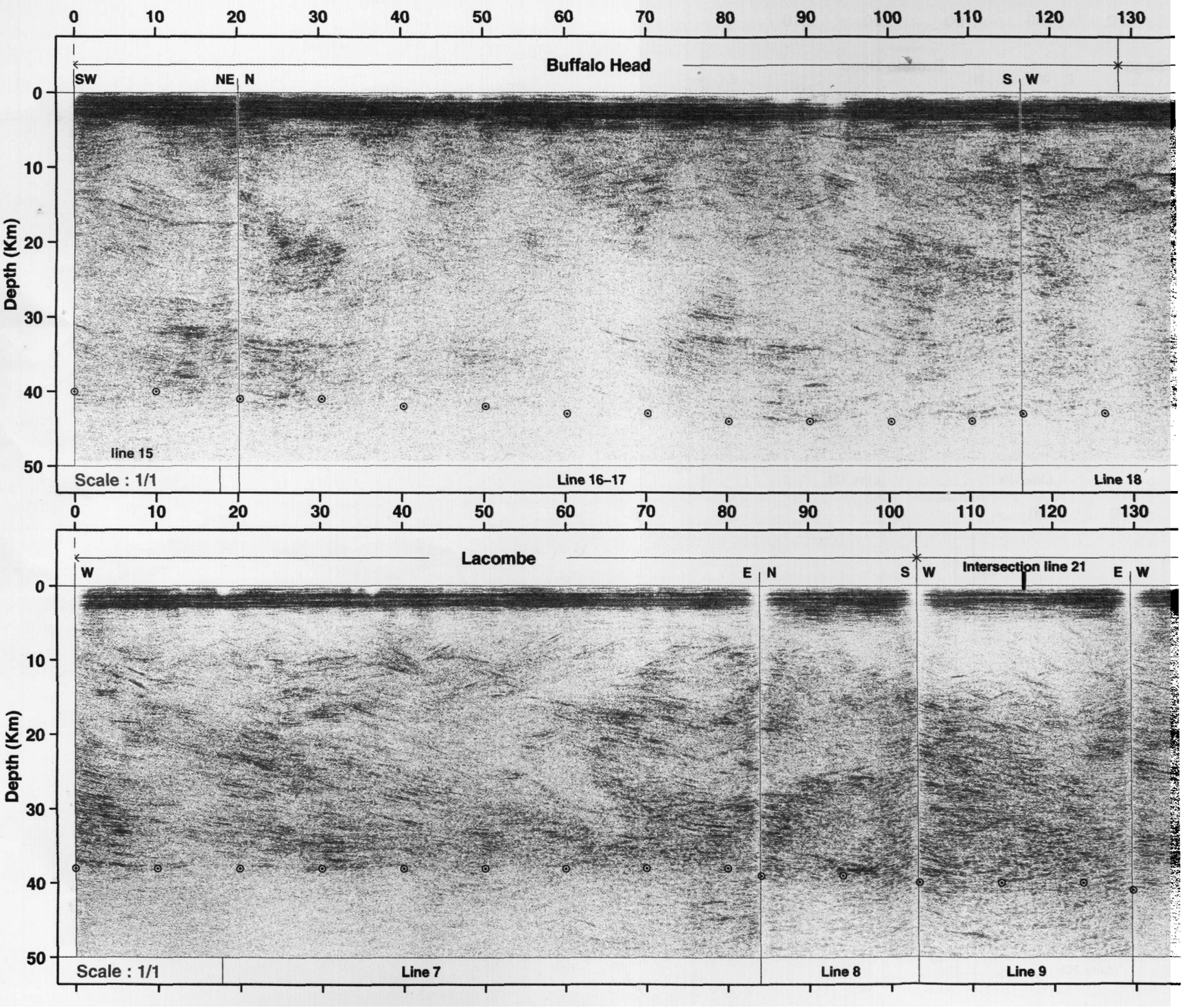

ead, Wabamun, Thorsby, Rimbey, Lacombe, Loverna, and Eye Hill domains.

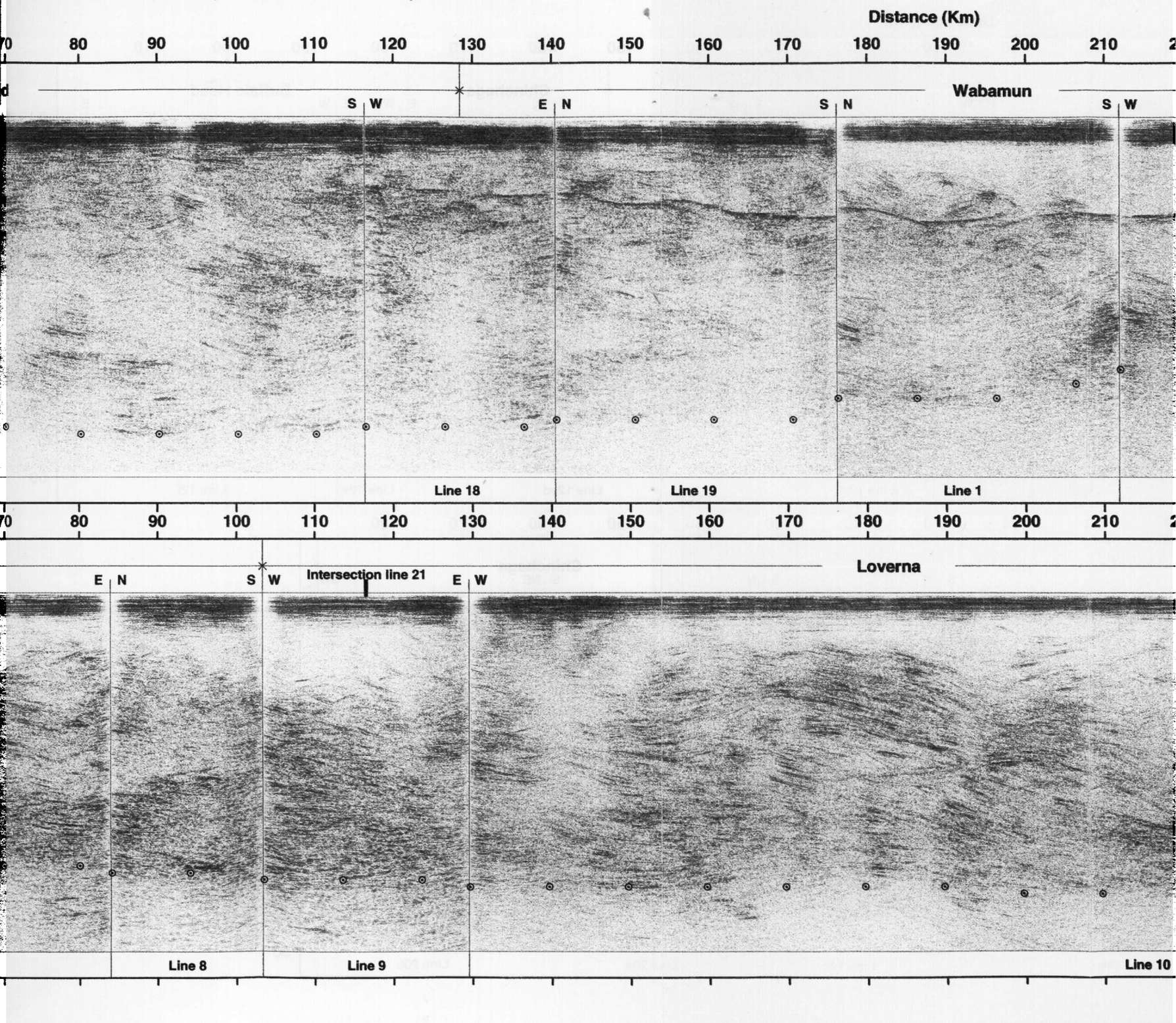

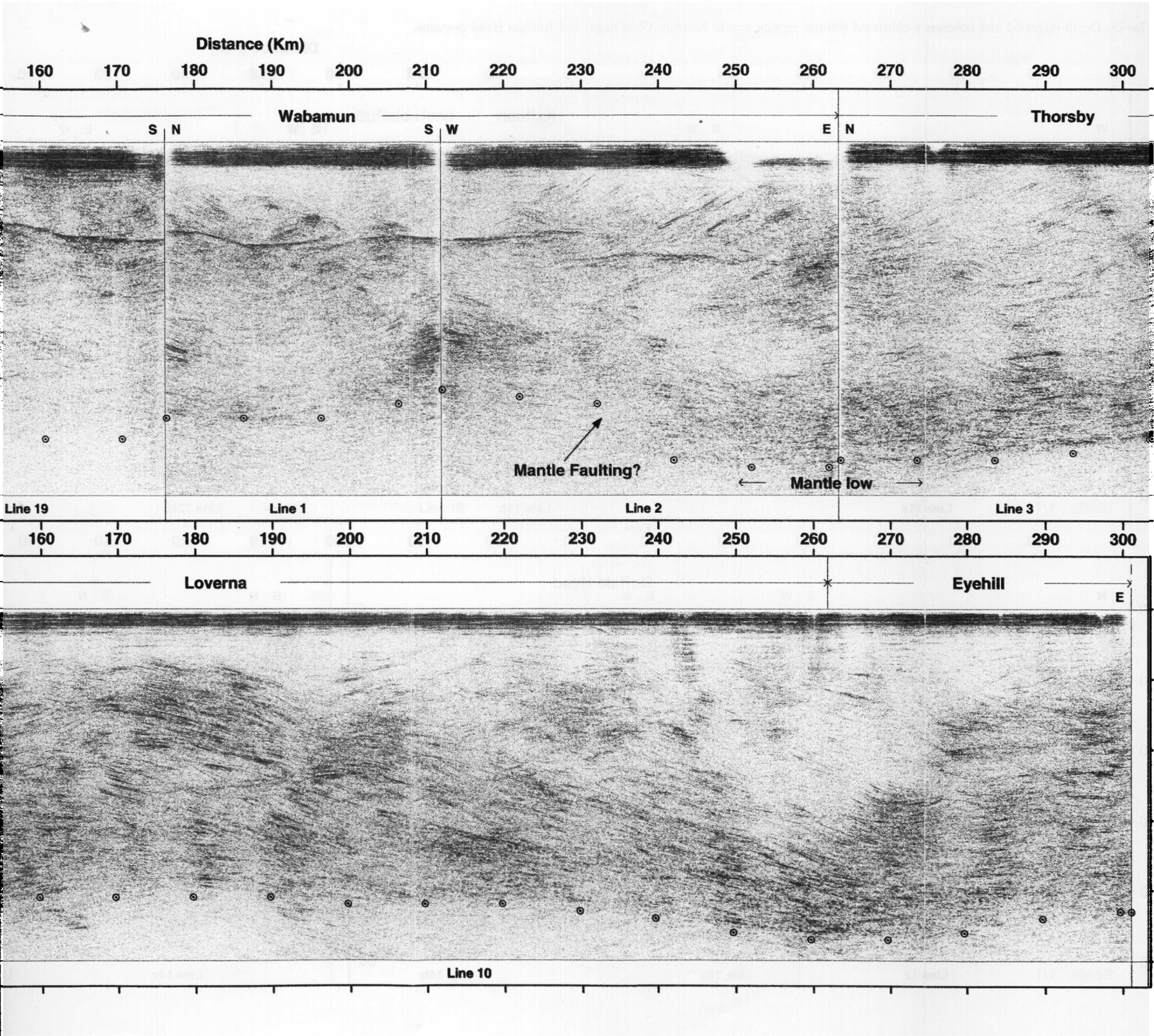

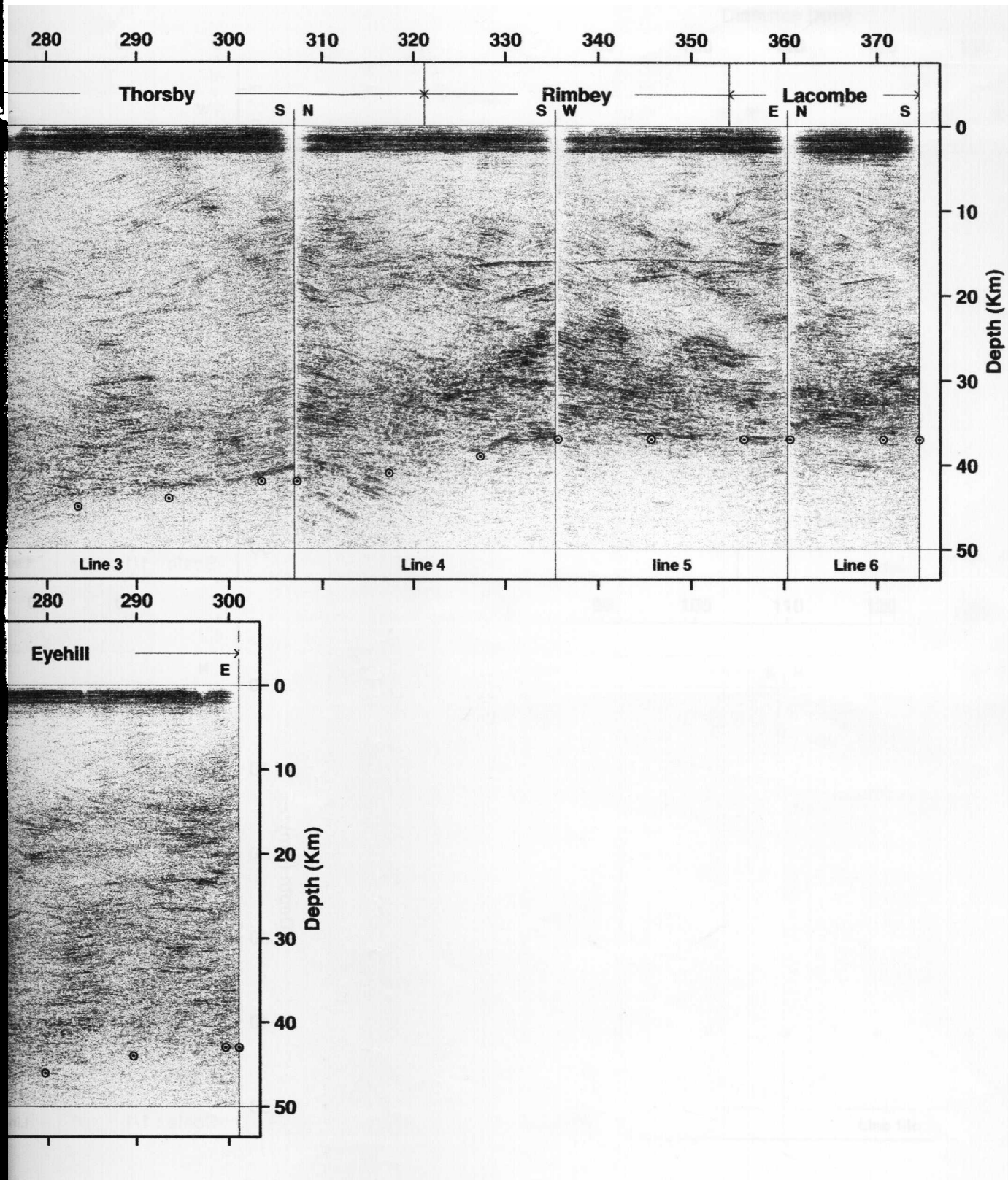

Fig. 6. Example of the final sedimentary velocity function employed for depth migration of line 23.

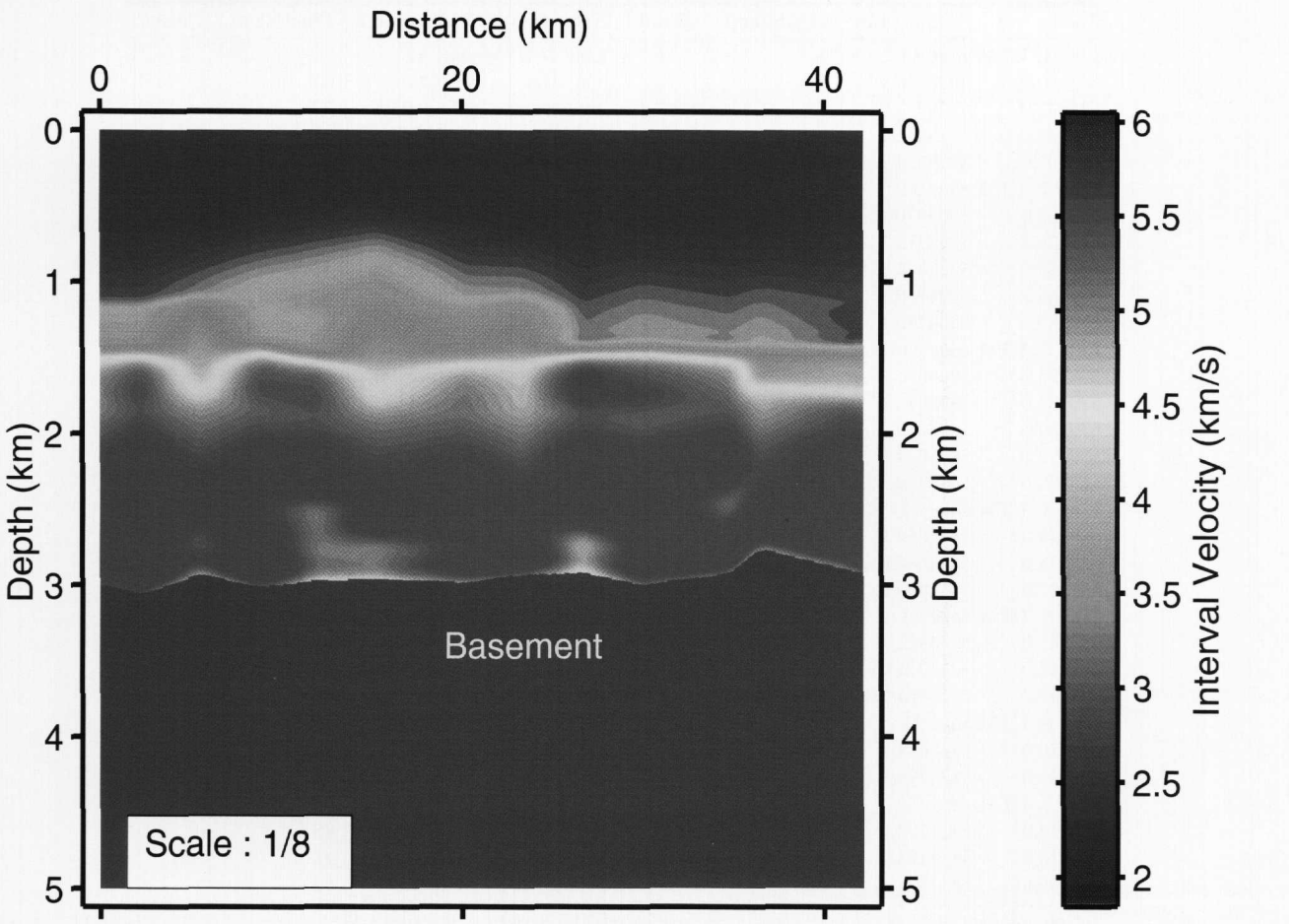

from variations in geologic structure to data acquisition problems. The character of the Moho in the profiles (Fig. 7) display this entire range of variability, and since this is so crucial to determining crustal thickness, it is important to discuss the character in detail.

Over the entire set of profiles, only one small section of less than 100 km length of class 1 Moho reflectivity is seen for short distances on CAT lines 3–5 between 280 and 360 km in Fig. 7*c*. This strong Moho also correlates with high reflectivity in the lower crust. The Mohorovičić discontinuity depths over much of these lines were picked along the sharp reflection, especially on line 5.

Class 2 Moho character dominates the profiles. Particularly good examples of this Moho type are seen on CAT lines 7–10 (Fig. 7*d*) where a reflectivity change is apparent along the entire length. Less distinct Moho character is seen in a number of locations especially those obtained in southernmost Alberta (lines 29–32), where the amplitudes slowly decrease with depth and no sharp change in character is seen. These lines cover Archean age crust (> 3 Ga), but it is unknown whether this is important for the lack of a clear Moho character. No crustal reflectivity is seen in lines 20a and 20b (Fig. 7*b*) below 20 km depth despite the clear class 2 Moho seen in line 14c only 30 km to the north. The reason for this is also unknown, but the rapid change in character from line 14 to line 20, both acquired as part of the PRAISE program but at different dates, may suggest the differences are due to changing acquisition conditions. This is the only section of all the profiles where the Moho cannot be reliably determined, and the values picked are extrapolated from the trend running from line 14. Acquisition differences may be further supported by the fact that the apparent upper crustal reflectivity (above 15 km) does not show the same level of detail seen in line 14. These observations highlight the care that must be taken when attempting to interpret observed variations in Moho reflectivity.

Despite these limitations, the reflection Moho is well defined over most of the profiles and its depth readily determined to better than a kilometre on the section (Tables 2–4). However, these values have been rounded to the nearest integer kilometre in recognition that the depth errors introduced by the velocity function used in the migration process are likely to be at most 2 km as noted earlier.

The observed Moho depths below sea level are combined with earlier refraction studies (Fig. 8) in the Peace River region (Halchuck and Mereu 1990), in southern Alberta (Kanasewich et al. 1969; Burianyk et al. 1997), and in western Alberta near the Rocky Mountains (Mereu et al. 1977). The crust over much of the study region is relatively thick near 40 km. The refraction results for the Peace River Arch region show local thickening along a northeastern-trending axis north of the Arch, whereas local crustal thinning is seen along line 12 (Fig. 7*a*), a model for this thinning will be presented later. Rapid changes in the crustal thickness appear in the vicinity

Table 2. Estimated depth to Moho below sea level of the CAT lines.

Easting (m)	Northing (m)	Depth (km)	Quality	Easting (m)	Northing (m)	Depth (km)	Quality
Line 1. UTM zone 11				**Line 7. UTM zone 12**			
635150.0	5938970.9	38	i	336504.0	5834494.1	37	c
635433.0	5928978.9	38	i	346494.0	5834190.9	37	c
635722.0	5918982.9	38	i	356487.0	5833824.9	37	c
636483.0	5909054.9	36	i	366484.0	5833596.1	37	c
Line 2. UTM zone 11				376480.0	5833316.9	37	c
635118.0	5905070.1	34	i	386478.0	5833082.1	37	c
645134.0	5905372.1	35	i	**Line 8. UTM zone 12**			
655085.0	5905678.9	36	i	388844.0	5834496.1	38	c
675763.0	5904780.1	45	i	**Line: 9. UTM zone: 12**			
674389.0	5904730.1	45	i	386900.0	5816866.9	39	c
Line 3. UTM zone 11				396898.0	5816662.1	39	c
678785.0	5908036.1	44	c	406896.0	5816456.9	39	c
679185.0	5898044.1	44	c	**Line 10. UTM zone 12**			
679569.0	5888050.9	44	c	411266.0	5817132.1	40	c
680172.0	5878074.9	43	c	417927.0	5814028.9	40	c
688489.0	5873230.9	41	c	427213.0	5816146.1	40	c
Line 4. UTM zone 11				436040.0	5813712.1	40	c
688449.0	5872068.1	41	c	445782.0	5812772.1	40	c
688838.0	5862082.9	40	c	454025.0	5815660.9	40	c
689222.0	5852090.9	38	c	464016.0	5815670.9	40	c
Line 5. UTM zone 11				474016.0	5815620.1	41	c
687965.0	5845322.1	36	c	484006.0	5815408.1	41	c
697956.0	5845754.9	36	c	489614.0	5809260.1	41	c
707864.0	5846594.9	36	c	499595.0	5809112.9	42	c
Line 6. UTM zone 11				509390.0	5810340.9	43	c
635150.0	5848684.1	36	c	518738.0	5812370.1	45	c
713576.0	5838796.1	36	c	528723.0	5812478.9	46	c
Line 7. UTM zone 7				537083.0	5815686.9	46	c
306524.0	5835590.1	37	c	547083.0	5815722.9	45	c
316518.0	5835238.9	37	c	557043.0	5815638.9	43	c
326509.0	5834834.1	37	c	566036.0	5816002.9	42	c

Note: Quality of Moho pick: c, clear; i, intermediate. UTM, Universal Transverse Mercator.

of the Snowbird tectonic zone on lines 1 through 5. Following earlier work (Ross et al. 2000), more than 10 km of Mohorovičić discontinuity topography is interpreted in line 2 beneath km 240 (Fig. 7*c*). We note that the seismic profiles do not demand this interpretation, and the Moho could be placed deeper at this location. However, this interpretation is not inconsistent with the corresponding gravity profiles as discussed in more detail later. In southern Alberta, the crust is generally thicker (>43 km; Figs. 7*g*, 7*h*) but is also more complex with a number of short-wavelength (~ 50 km) features. The most prominent is the Vulcan structure at km 100 on line 25 (Fig. 7*f*), which displays nearly 7 km of Moho topography with an axis of thickening between lines 25 and 32 along the Vulcan low, as defined in the potential-field maps.

Geological interpretation

The thickness of the crust can be an important diagnostic indicator of crustal history, with thinning and thickening generally indicating extension or compression, respectively, (Mooney and Meissner 1992). In this section we interpret three of the more significant thickness anomalies in Alberta.

Spirit River mantle high

Lines 11 and 12 of the PRAISE 94 survey (Fig. 7*a*) confirm the existence of a 50 km wide crustal thin with a Moho elevation of less than –38km. We suggest the name Spirit River mantle high for this feature, after Imperial Spirit River No. 1, one of the early exploratory wells in the area (Fig. 9).

The Kimiwan isotopic anomaly (KIA) has been discussed at length by Burwash et al. (2000*b*). The formation of KIA between 1800 and 1700 Ma is attributed to crustal extension at that time, primarily along the Kimiwan and Dunvegan faults (Fig. 9). The half-graben then formed corresponds to the Chinchaga low and the west flank of the Buffalo Head terrane (Villeneuve et al. 1993). Core samples from this northwest-trending aeromagnetic low are amphibolite facies, often overprinted by epidote-amphibolite- to greenschist-facies hydrothermal alteration. Core recovered from Imperial Belloy No. 2 (Fig. 9) is gneissic granulite (Burwash et al. 2000*a*), indicating uplift of the Dunvegan fault block. High magnetic susceptibilities were measured for a number of cores west of the Dunvegan fault. These include Imperial Belloy No. 2, 2300×10^{-6} emu/cm^3 and Phillips Ksituan No. 1, 3900×10^{-6} emu/cm^3 (deformed quartz monzonite augen gneiss, U–Pb age 1986 Ma, Villeneuve et al. 1993). The high magnetic susceptibilities are reflected in the Ksituan aeromagnetic high.

The Spirit River mantle high, which underlies part of the Ksituan domain, occurs down the projection of the Kimiwan

Figs. 7*e*–7*f*. Depth-migrated and coherency-enhanced seismic section across Loverna and Medicine Hat domains, and the Vulcan Low.

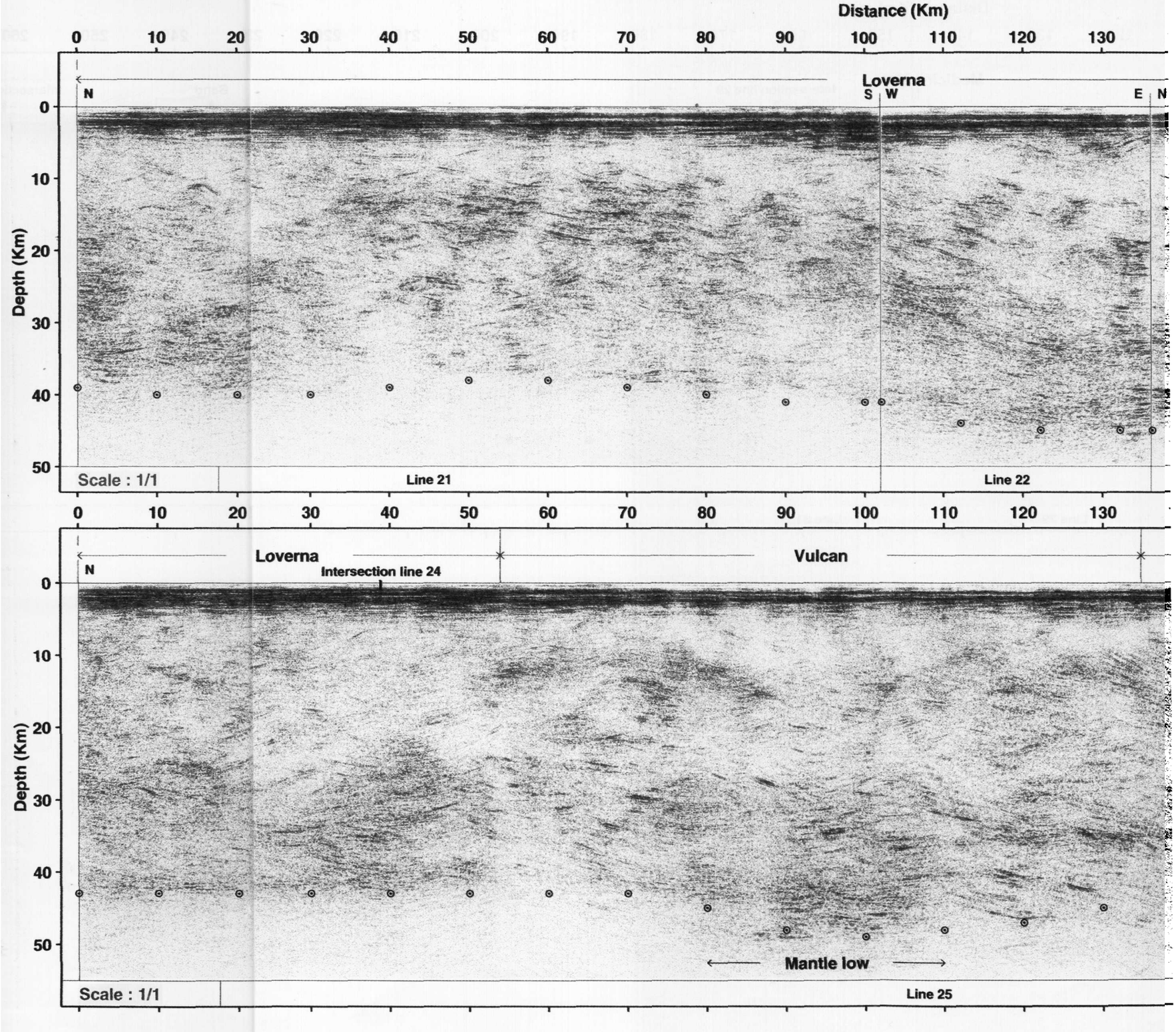

and the Vulcan Low.

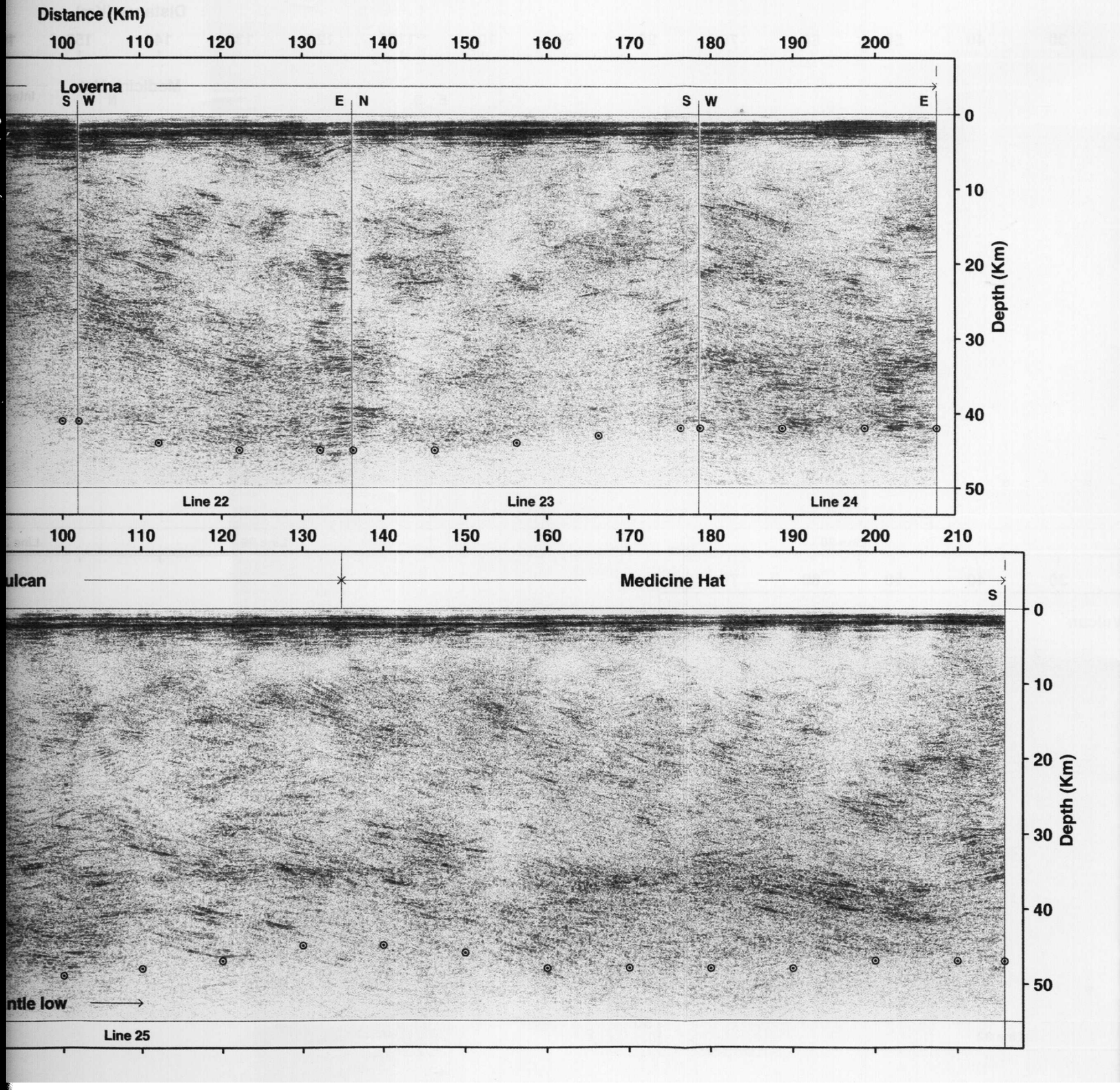

Figs. 7*g*–7*h*. Depth-migrated and coherency-enhanced seismic section across Medicine Hat and the Vulcan Low.

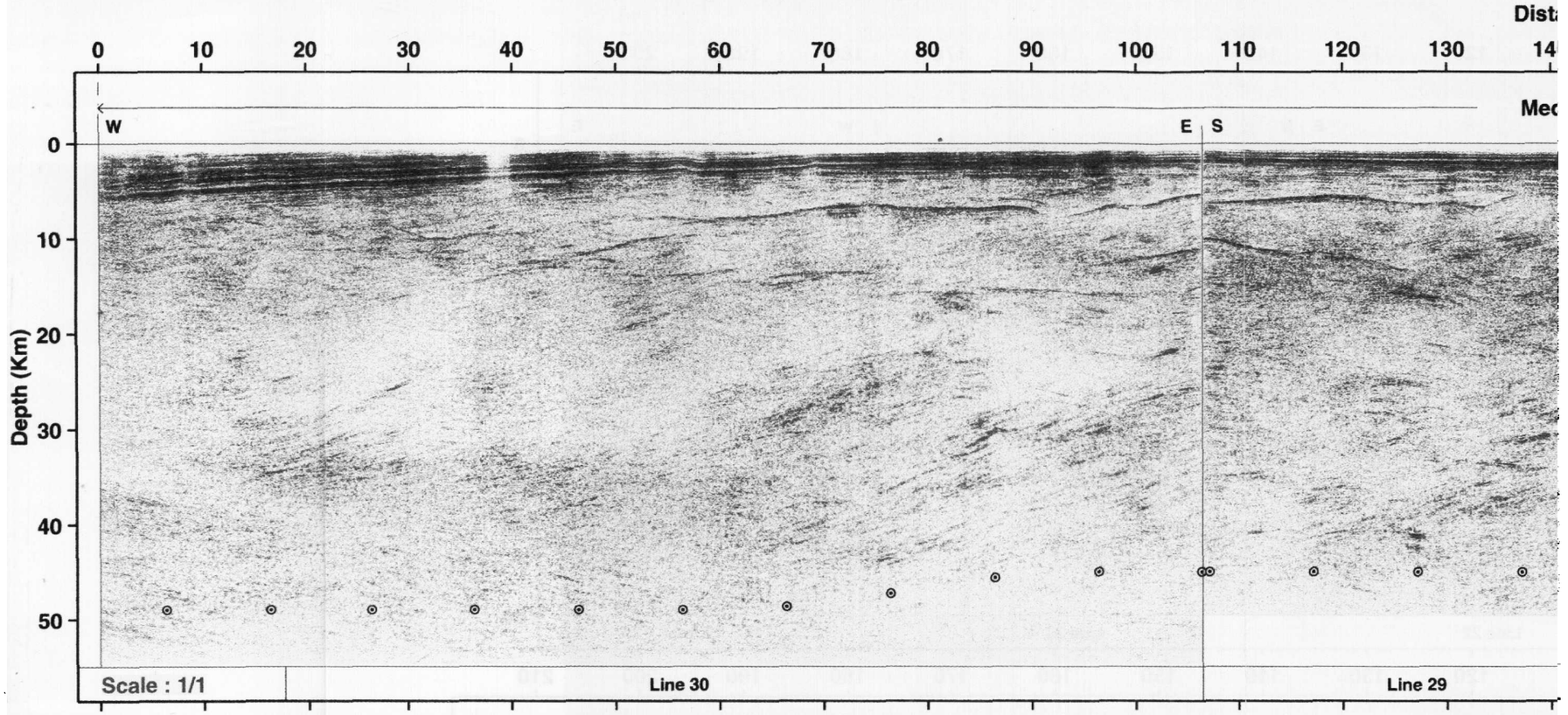

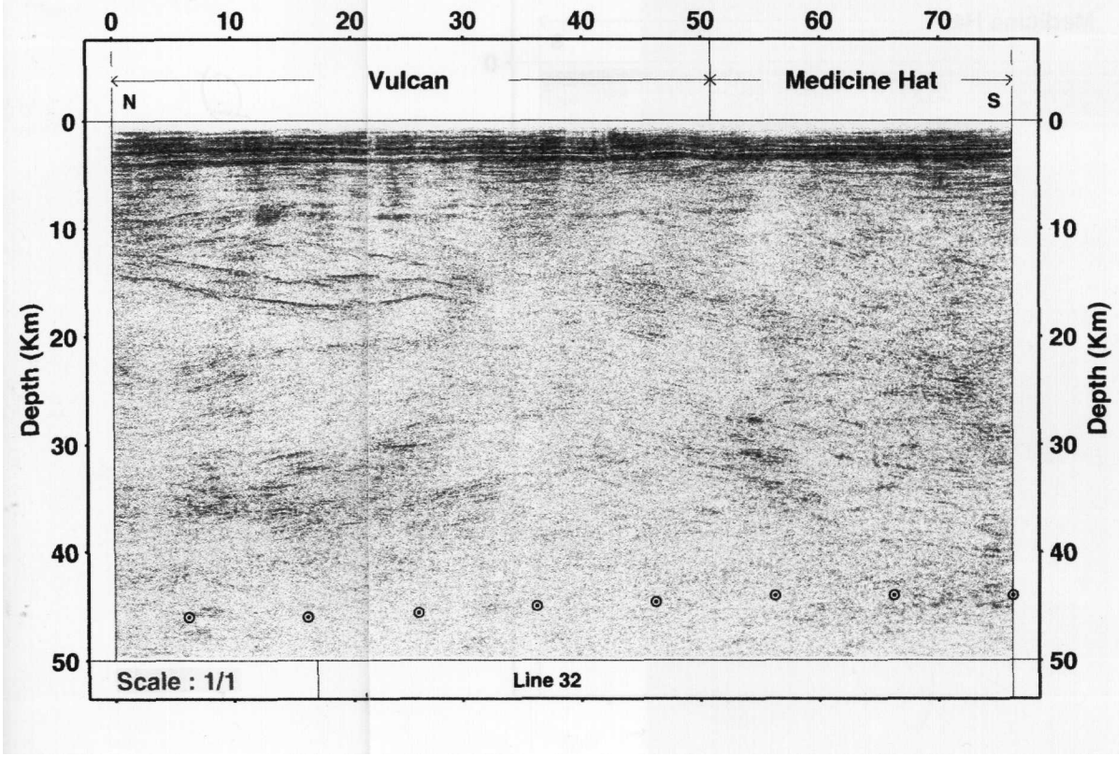

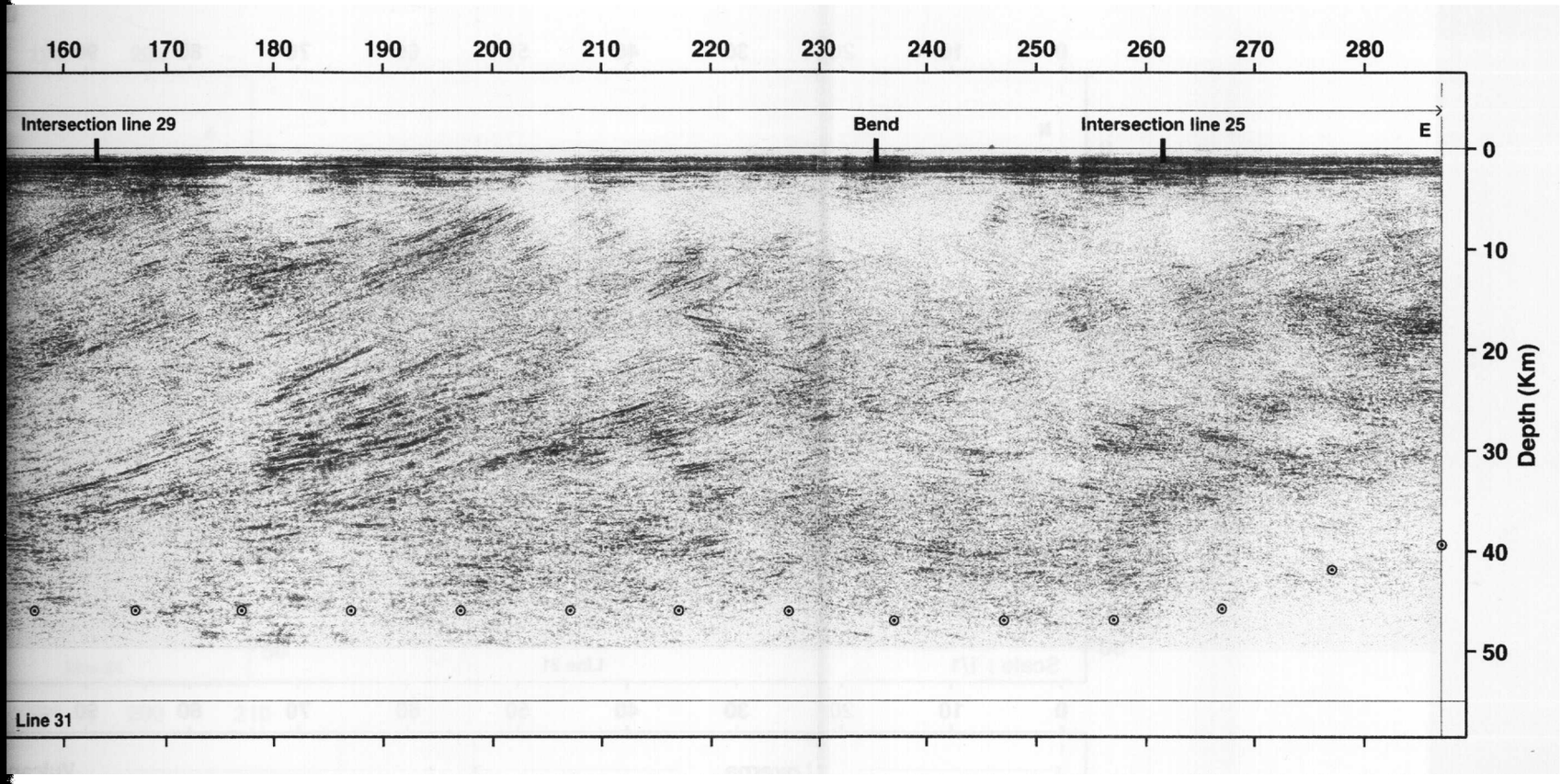

Table 3. Estimated depth to Moho below sea level of the PRAISE lines.

Easting (m)	Northing (m)	Depth (km)	Quality	Easting (m)	Northing (m)	Depth (km)	Quality
Line 11a. UTM zone 11.				**Line 14b. UTM zone 11**			
280984.0	6201306.9	39	c	520411.0	6147256.9	40	c
290735.0	6199948.1	39	c	520708.0	6147006.9	40	c
300683.0	6199116.1	39	c	520566.0	6137412.1	40	c
310641.0	6199050.1	39	c	519424.0	6127536.9	40	c
320135.0	6198256.1	39	c	519608.0	6117540.9	40	c
330127.0	6197852.1	39	c	518433.0	6107724.1	40	c
Line 11b. UTM zone 11				**Line 14c. UTM zone 11**			
332766.0	6194506.1	40	c	509756.0	6097092.9	40	i
342759.0	6194134.9	40	c	510370.0	6087156.1	40	i
352753.0	6193798.9	39	c	514363.0	6077992.9	40	i
362662.0	6193000.1	38	c	**Line 15. UTM Zone 11**			
372488.0	6193220.9	37	c	593748.0	6068518.9	39	i
382429.0	6193720.1	37	c	602174.0	6073228.9	39	i
Line 12ab. UTM zone 11				**Line 16–17. UTM zone 11**			
383687.0	6189606.1	37	c	595175.0	6067972.9	40	i
393684.0	6189360.9	37	c	596002.0	6058024.9	40	i
403653.0	6189444.9	37	c	595581.0	6048276.9	41	i
Line 12cd. UTM zone 11				594621.0	6038380.9	41	i
414917.0	6185626.1	38	c	592932.0	6028616.9	42	i
424915.0	6185428.1	38	c	597013.0	6020314.9	42	i
434913.0	6185264.1	38	c	601207.0	6011478.1	43	i
444912.0	6185128.1	38	c	604616.0	6002346.1	43	i
454912.0	6185014.9	38	c	604661.0	5992698.9	43	i
Line 12x. UTM zone 11				604083.0	5982774.1	43	i
458488.0	6188218.9	38	c	**Line 18. UTM zone 11**			
Line 12f. UTM zone 11				604568.0	5976846.9	42	i
468276.0	6184900.1	39	c	614108.0	5975684.1	42	i
478288.0	6184834.1	40	c	624105.0	5975912.9	42	i
488288.0	6184792.9	40	c	**Line 19. UTM zone 11**			
498288.0	6184778.1	40	c	628606.0	5974880.1	41	i
Line 13. UTM zone 11				628893.0	5964884.9	41	i
501567.0	6187950.9	40	c	629500.0	5954952.9	41	i
501584.0	6177950.9	40	c	631722.0	5945466.9	41	i
501582.0	6167950.9	40	c	**Line 20a. UTM zone 11**			
503213.0	6158214.1	40	c	510704.0	6055926.9	?	u
503219.0	6148214.1	40	c	512955.0	6051462.9	?	u
Line 14a. UTM zone 11				513752.0	6046716.9	?	u
500812.0	6149152.1	40	c	**Line 20b. UTM zone 11**			
510790.0	6149528.9	40	c	508675.0	6029098.9	?	u
5204110	6147256.9	40	c	504241.0	6027030.9	?	u
				499754.0	6024928.9	?	u

Note: Quality Moho pick: c, clear; i, intermediate; u, undefined. UTM, Universal Transverse Mercator.

fault plane (Fig. 9). We infer that this north-trending mantle high (Stephenson et al. 1989) is related to the Paleoproterozoic extension during which KIA was formed.

A Phanerozoic analogue of the KIA is found in the $\delta^{18}O$-depleted rocks exposed along the east side of the Okanagan Valley in southern British Columbia (Nesbitt and Muehlenbachs 1995). There, hydrothermally altered rocks are associated with the low-angle, westward dipping Okanagan Valley fault (OVF), a 50 Ma extensional feature (Parrish 1992). A mantle high (Cook 1995) with associated Eocene andesitic volcanism (Marron Formation) occurs 120 km west of and parallel to the OVF. High heat flows still persist along OVF (Hyndman and Lewis 1995). We believe that the Eocene extensional OVF, $\delta^{18}O$ depletion and Marron mantle high are valid models for KIA and the Spirit River mantle high.

Edmonton mantle low

The 1992 Central Alberta Transect crosses three major basement domains in east-central Alberta (Fig. 10), each characterized by a separate range of U–Pb ages (Ross et al. 1991). The Athabasca Polymetamorphic Terrane (APT, Burwash et al. 1993), with a 1.9 to 2.4 Ga range of U–Pb zircon, monazite, and titanite ages, lies to the northwest of a major crustal lineament marked by paired Bouguer gravity high and low trends (FdL, Fond du Lac low of Walcott and Boyd 1971). This lineament was referred to by Burwash and Culbert (1976) as the Edmonton – Kasba Lake line and by Hoffman (1988) as the Snowbird line.

Southeast of the FdL (Figs. 3, 10), U–Pb ages change abruptly to less than 1.9 Ga at four dated localities (the Rimbey magmatic arc of Ross et al. 1991). Burwash and Muehlenbachs (1997) refer to the core samples of

Table 4. Estimated depth to Moho below sea level of the SALT lines.

Easting (m)	Northing (m)	Depth (km)	Quality	Easting (m)	Northing (m)	Depth (km)	Quality
Line 21. UTM zone 12				**Line 25. UTM zone 12**			
399879.0	5818206.0	38	c	459013.0	5548894.0	47	c
398320.0	5808542.0	39	c	463822.0	5540979.0	47	c
397820.0	5798584.0	39	c	464661.0	5531096.0	46	c
397295.0	5788622.0	39	c	467505.0	5521556.0	46	c
397088.0	5778624.0	38	c	**Line 29. UTM zone 12**			
395245.0	5768947.0	37	c	395989.0	5505800.0	45	i
395939.0	5759126.0	37	c	395811.0	5495802.0	44	i
397920.0	5749859.0	38	c	396291.0	5485852.0	44	i
397643.0	5739869.0	39	c	396588.0	5475890.0	44	i
397463.0	5729871.0	40	c	396398.0	5465892.0	44	i
397145.0	5719881.0	40	c	**Line 30. UTM zone 12**			
Line 22. UTM zone 12				398119.0	5473410.0	44	i
395608.0	5719606.0	40	c	388609.0	5475934.0	44	i
405599.0	5719412.0	43	c	378834.0	5477035.0	44	i
415592.0	5719245.0	44	c	368838.0	5477172.0	45	i
425542.0	5719091.0	44	c	358853.0	5477512.0	47	i
Line 23. UTM zone 12				348944.0	5477848.0	48	i
426660.0	5720453.0	44	c	338948.0	5478125.0	48	i
427619.0	5710744.0	44	c	328952.0	5478415.0	48	i
427500.0	5700745.0	43	c	319570.0	5478935.0	48	i
427367.0	5690750.0	42	c	310781.0	5480636.0	48	i
427084.0	5680760.0	41	c	300895.0	5479776.0	48	i
Line 24. UTM zone 12				**Line 31. UTM zone 12**			
425647.0	5680227.0	41	c	506284.0	5524337.0	36	i
435642.0	5680091.0	41	c	496284.0	5524350.0	39	i
445637.0	5679965.0	41	c	486284.0	5524367.0	41	i
Line 25. UTM zone 12				476288.0	5524323.0	45	i
453730.0	5718706.0	42	c	467057.0	5520748.0	46	i
453645.0	5708656.0	42	c	457283.0	5519391.0	46	i
453541.0	5698656.0	42	c	451479.0	5513048.0	46	i
453452.0	5688657.0	42	c	448233.0	5505155.0	45	i
454959.0	5678891.0	42	c	438233.0	5505256.0	45	i
457531.0	5669376.0	42	c	428234.0	5505376.0	45	i
458870.0	5659583.0	42	c	418235.0	5505518.0	45	i
460541.0	5649865.0	42	c	408236.0	5505678.0	45	i
459544.0	5640015.0	44	c	399455.0	5502659.0	45	i
455150.0	5631514.0	47	c	389458.0	5502763.0	45	i
451441.0	5623904.0	48	c	**Line 32. UTM zone 12**			
452976.0	5614154.0	47	c	307121.0	5531067.0	43	d
452900.0	5604154.0	46	c	307646.0	5541074.0	43	d
453276.0	5594215.0	44	c	307882.0	5550595.0	43	d
450310.0	5585592.0	44	c	306577.0	5560302.0	43	d
450221.0	5575592.0	45	c	306767.0	5570296.0	44	d
450283.0	5565605.0	47	c	310249.0	5579130.0	44	d
452809.0	5556495.0	47	c	310610.0	5589123.0	45	d
				310973.0	5599117.0	45	d

Note: Quality of Moho pick: c, clear; i, intermediate; d, diffuse. UTM, Universal Transverse Mercator.

leucocratic granitic rocks of this area as the Central Alberta Intrusions (CAI). Farther east along FdL lies the 1820 Ma Junction granite (Bickford et al. 1986), which is exposed in the La Loche map area, NTS 74 C (Fig. 10). The CAI domain is transitional into the Archean Southern Alberta Craton (SAC). The high-angle Warburg thrust fault (Wb in Fig. 10), was first identified by Ross et al. (1995) and named by Burwash and Muehlenbachs (1997). Figure 11 presents gravity, seismic, and geologic cross-sections along lines A–A′, B–B′, and C–C′. The interpretations given below are based on Figs. 10 and 11 together with petrologic and geophysical characteristics of the sample populations from the three domains shown in Table 5.

Gravity profiles

A paired gravity high and low normally mark the transition from a crustal region of higher average density to one of lower density. Table 5 indicates that the average density of samples of APT (n = 13) and CAI (n = 8) shown on Fig. 10 are 2.72 vs. 2.64, respectively. The higher density of APT reflects a higher mafic mineral content, lower SiO_2 and therefore lower quartz content. The CAI rock suite is composed predominantly of leucocratic granites and quartz monzonites. This change of mafic content was noted by Garland and Burwash (1959), who recognised but did not name the Fond du Lac Bouguer gravity high northwest of Edmonton.

The plane separating the terranes of contrasting density is

Fig. 8. Depth to the Mohorovičić discontinuity as measured from orthometric sea level. Refraction results incorporated include Halchuk and Mereu (1990) in the northwest; Kanasewich et al. (1969) and Burianyk et al. (1997) in the south; and Mereu et al. (1977) in western Alberta at the Rocky Mountains. Locations of mantle topographic features discussed later in the text include the Spirit River mantle high, the Edmonton mantle low within the Snowbird tectonic zone, and the Vulcan mantle low.

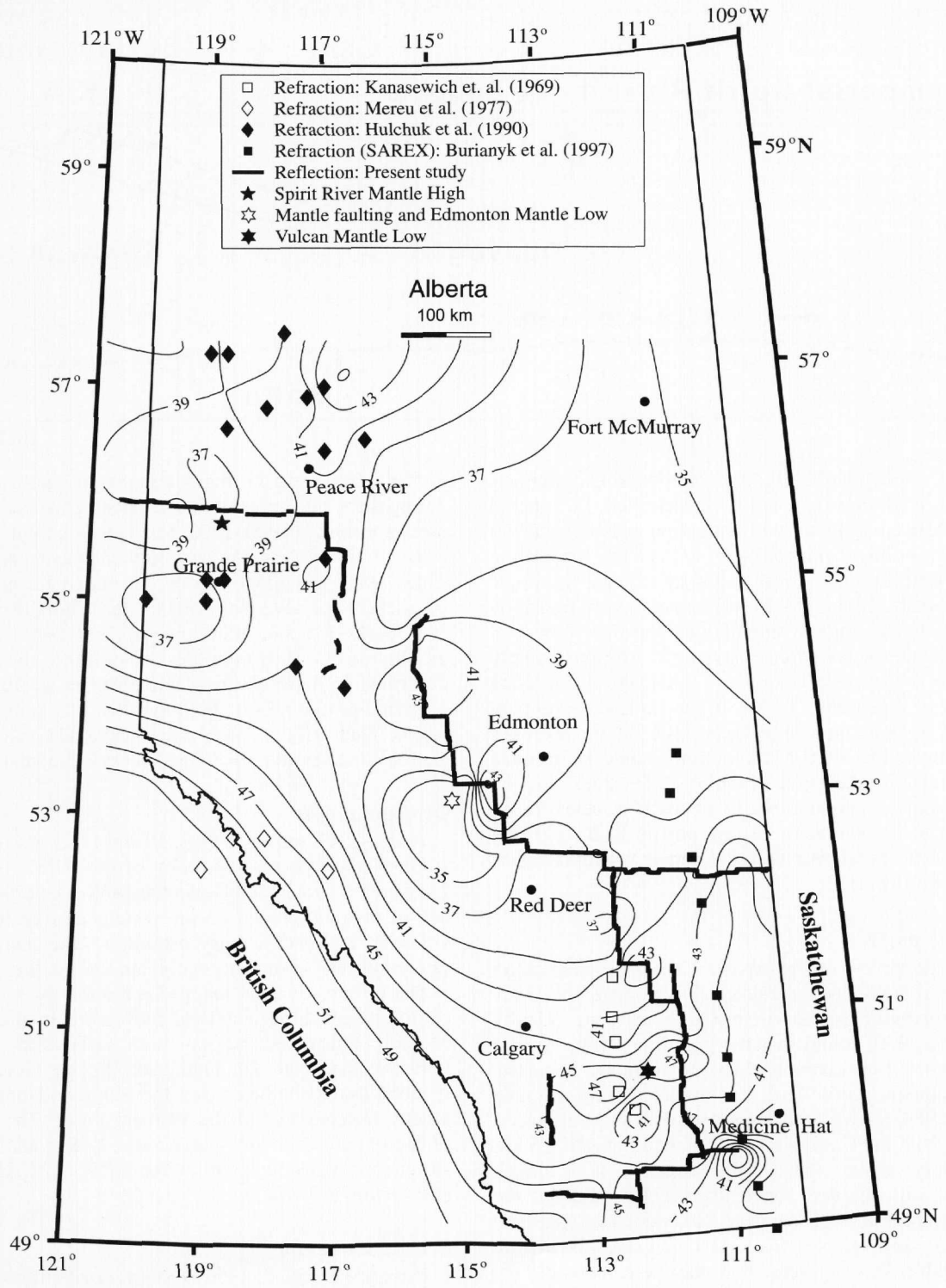

the Warburg thrust fault (Fig. 6, Burwash and Muehlenbachs 1997). Using time-migrated data, Ross et al. (Fig. 3, 1995) located Wb as a major feature on CAT line 2. Their interpreted section shows an upward curvature on the Moho north of the fault. The shallower depth to Moho is also a factor in the strong positive anomaly of the Fond du Lac high. Crustal thinning north of the thrust is reflected by a change of regional metamorphic facies. North of Wb, rocks range from upper amphibolite to granulite facies (Fig. 1, Burwash et al. 2000*a*). Two of the wells, marked with asterisks

Fig. 9. Inferred Crustal structure across Ksituan–Chinchaga–Buffalo Head domains; PRAISE 94 line 11(west half) and line 12. Kimiwan, Dunvegan and minor faults from Burwash, et al. (2000*b*). Crustal thinning across zone 50 km wide is on down-dip projection of Kimiwan extensional faulting below Chinchaga half-graben. KIA is the Kimiwan isotopic anomaly. Imperial (I.) Belloy 2 core sample of gneissic granulite marks edge of the Dunvegan horst.

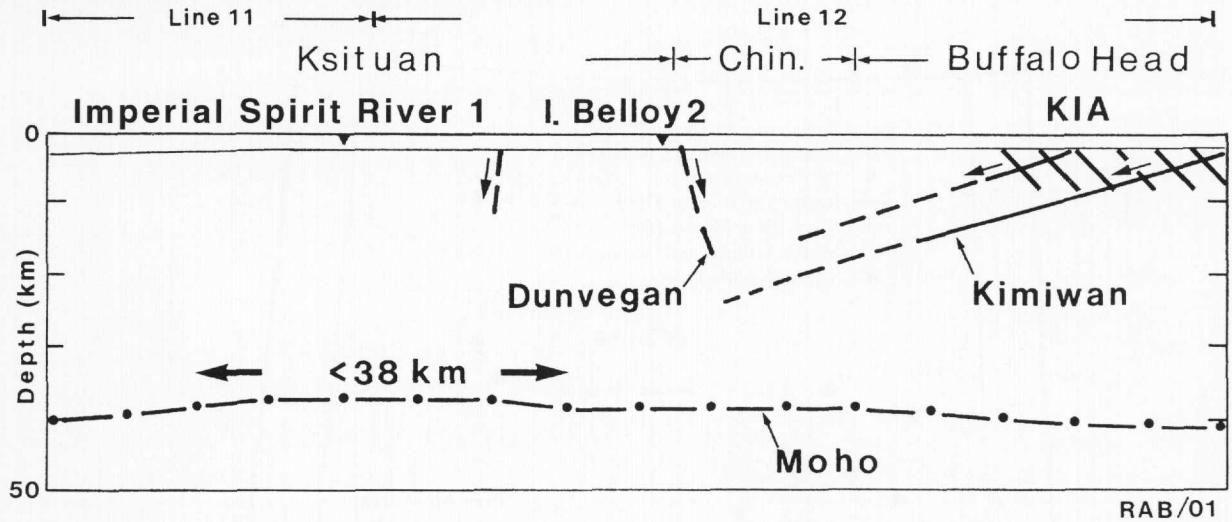

on Fig. 10, penetrated orthopyroxene-bearing gneisses. South of Wb, granulites have not been identified. In Imperial Leduc No. 530, continuous core sampling was carried out from the Cambrian cover rocks 5 m into the crystalline basement. From the unconformity downward, the lithologic sequence is weathered granite, fresh granite, a sharp transition to fresh amphibolite, epidote amphibolite, and finally, at total depth, greenschist-facies supracrustal rock. The most likely interpretation is that an offshoot of a small pluton intruded country rock of greenschist facies. In the La Loche National Topographic System map area NTS 74C, on the exposed Canadian Shield, the 1820 Ma Junction granite is intruded along the boundary between granulite-facies rocks to the northwest and lower amphibolite- to greenschist-facies Virgin River schists to the southeast. Along profile B–B′, a strong gravity high reflects faulting with the denser granulite-facies rocks to the northwest.

Aeromagnetic profiles

Aeromagnetic surveys on the exposed Canadian Shield reflect rapid lateral variation in near-surface rock type more effectively than gravity surveys. Near the Virgin River shear zone (VRSZ), Wallis (fig. 5, 1970) found that the granulite terrane Lisgar Lake high showed an extreme range of magnetic response. The B–B′ magnetic profile (Fig. 11) prepared from the map of Agarwal (1968) shows similar variation over short distances. Along A–A′, with the Canadian Shield buried beneath 2.5 km of sedimentary cover, the profile over APT is much smoother but still elevated above the average value of the CAI. The average values of magnetic susceptibilities measured over basement core samples from APT and CAI show little difference (Table 4). One factor that may be responsible for the high, therefore, is the shallower depth to mafic mid-crustal rocks.

The Thorsby low (Ross et al. 1991) lies above the footwall zone of the Warburg thrust. Watanabe (1965) cut core samples of the mylonitic rocks across the north–south-trending Charles Lake shear zone in northeastern Alberta. He determined that mylonization along this major transcurrent fault zone, especially during the waning amphibolite to greenschist facies of regional metamorphism, 1900–1800 Ma (McDonough et al. 2000), resulted in rocks with very low magnetic susceptibilities. These rocks are identified on aeromagnetic maps as linear magnetic lows. We believe that the Thorsby aeromagnetic low marks a major transcurrent shear zone. The Junction granite (profile B–B′) intrudes mylonites of the VRSZ and is deformed by later shearing (Bickford et al. 1986). The flat magnetic profile reflects both the shearing and the leucocratic pluton. Wallis (fig. 5, 1970) also found a relatively flat magnetic response across the VRSZ and metasedimentary belt.

Geologic profile

Profile C–C′, shown on Figs. 10 and 11, is based on a detailed study of the structural geology of the VRSZ in the Careen Lake area (Carolan and Collerson 1988). A northeast-trending belt of mylonitic rocks 4.5 km wide is derived from plutonic, volcanic, and sedimentary protoliths. The metasedimentary mylonites are compositionally similar to the Virgin River Schist Group. Carolan mapped a number of kinematic indicators, establishing a dextral movement in the shear zone. Mineral lineations suggest both strike-slip and dip-slip (thrust) components. The high-grade Western Granulite Domain is thrust to the southeast over the Mudjatic Domain. This geometry matches that of the Warburg thrust. The juxtaposition of high-grade over low-grade rocks is also analogous to the structure that we suggest for the APT and CAI domains of east-central Alberta.

Crustal thickening

Ross et al. (Fig. 3, 1995) showed crustal thickening on the south-east side of the Warburg thrust. Their interpreted maximum crustal thickness, based on time-migrated data, is less than 40 km. The depth-migrated data for CAT lines 1–7 projected to cross-section A–A′ (Fig. 11) suggest a crustal thickness of up to 45 km. Between 1800 and 500 Ma (Upper Cambrian time), 8–10 km of upper crustal rocks,

Fig. 10. Precambrian domains of east-central Alberta surveyed by the Lithoprobe Central Alberta Transect (CAT) seismic lines. The Athabasca Polymetamorphic Terrane (APT, Burwash et al. 1993) with U–Pb ages 1.9 to 2.4 Ga lies to the northwest of the Fond du Lac (FdL) Bouguer gravity low. The Central Alberta Intrusions (CAI), with ages ranging from 1798 to 1856 Ma (Ross et al. 1991), flank the southeast side of FdL. The CAI domain is transitional into the Archean Southern Alberta Craton (SAC). The high-angle Warburg thrust fault (Wb, Burwash and Muehlenbachs 1997) was identified by Ross et al. (1995). Core samples from the two wells marked with an asterisk (*) are granulite-facies gneiss. Locations of cross-sections A–A′, B–B′, and C–C′ of Fig. 11 are shown. VR, Virgin River.

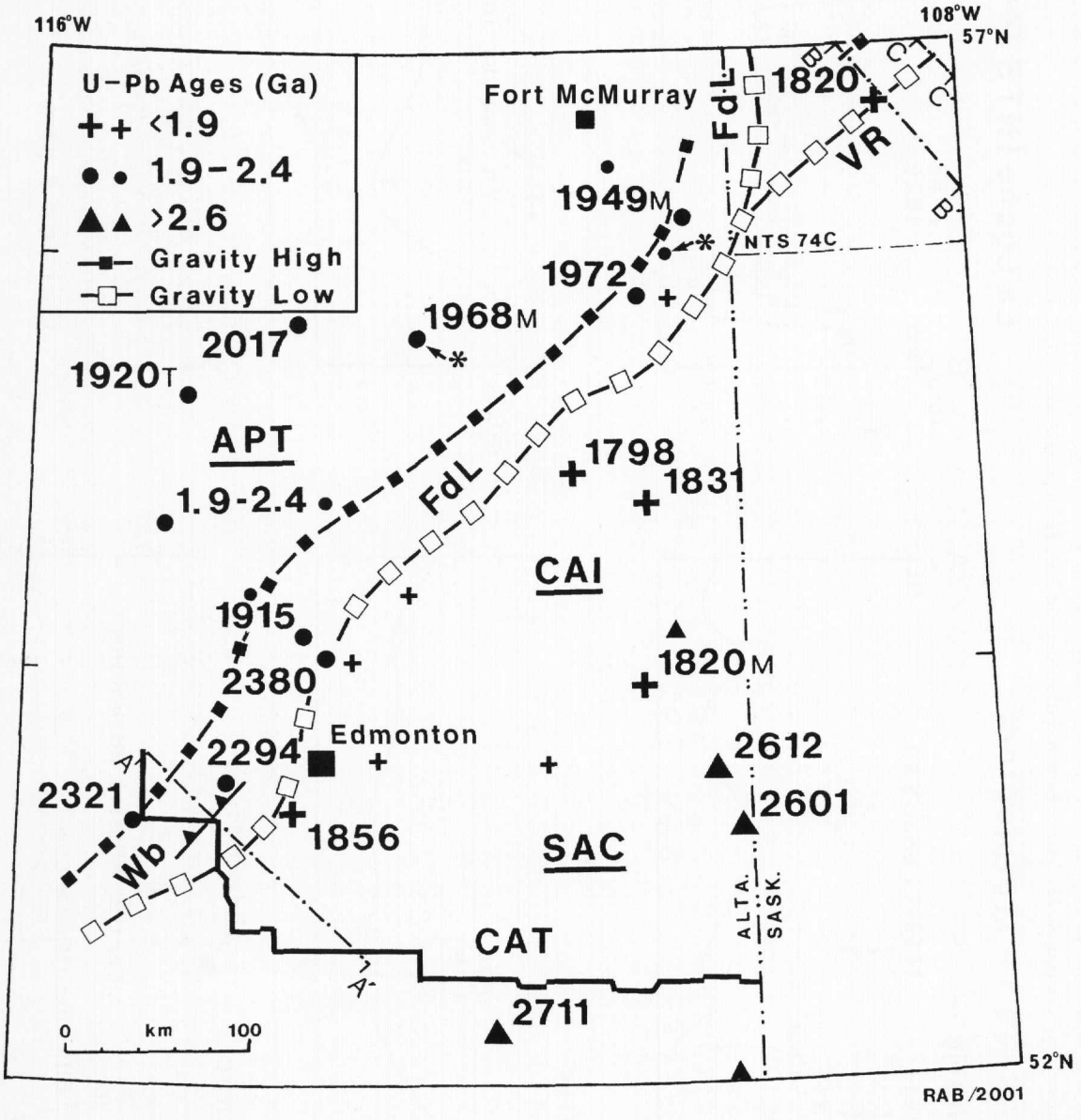

unmetamorphosed to lower amphibolite facies, were eroded in the Edmonton area. Therefore, after the compression that formed the Warburg thrust, ca.1800 Ma, the CAI domain would have been very thick, in the order of 55 km at the Edmonton mantle low.

In the Milk River area of southern Alberta, Davis et al. (1995) found that reheating of the 2.7 Ga SAC crust had occurred at approximately 1800 Ma. The evidence was provided by U–Pb ages of zircon from lower crustal xenoliths brought to the surface by the 50 Ma Sweet Grass intrusions. Burwash and Muehlenbachs (1997) interpreted the 1800 Ma thermal event as a reflection of the closure of the Manikewan suture zone 500 km to the east. Using this southern Alberta model, a 55 km thick crust in the Edmonton mantle low would have been subjected to anatectic melting. A series of mesozonal to epizonal plutons would have been emplaced in the upper crust, the Central Alberta Intrusions. Whole-rock major and trace element analyses (Burwash and Muehlenbachs 1997) support such an origin. On the exposed Canadian Shield, the granite body now known as the 1820 Ma Junction granite is described by Tremblay (1961) as a massive to faintly gneissic metasomatic granite, elongated parallel to the enclosing gneisses. This description also supports an origin by anatexis.

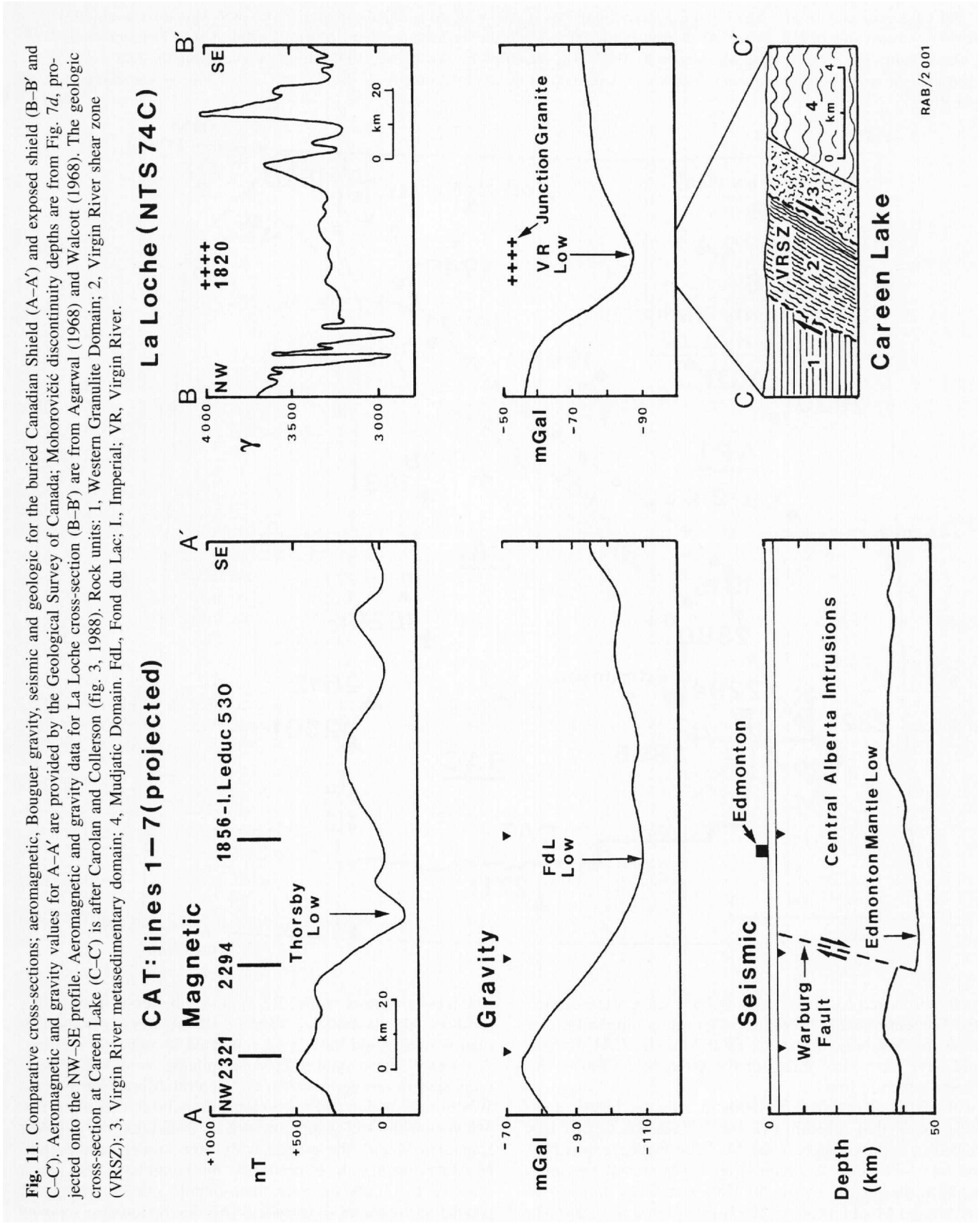

Fig. 11. Comparative cross-sections; aeromagnetic, Bouguer gravity, seismic and geologic for the buried Canadian Shield (A–A′) and exposed shield (B–B′ and C–C′). Aeromagnetic and gravity values for A–A′ are provided by the Geological Survey of Canada; Mohorovičić discontinuity depths are from Fig. 7*d*, projected onto the NW–SE profile. Aeromagnetic and gravity data for La Loche cross-section (B–B′) are from Agarwal (1968) and Walcott (1968). The geologic cross-section at Careen Lake (C–C′) is after Carolan and Collerson (fig. 3, 1988). Rock units: 1, Western Granulite Domain; 2, Virgin River shear zone (VRSZ); 3, Virgin River metasedimentary domain; 4, Mudjatic Domain. FdL, Fond du Lac; I., Imperial; VR, Virgin River.

Table 5. Comparison of Petrologic and Physical Characteristics of Basement Core Sample Suites from APT, CAI, SAC, and WCSB.

Domain vs. property	Mafic minerals (%)	SiO_2 (wt.%)	Specific gravity	Magnetic susceptibility (10^{-6}emu/cm3)
APT (n = 13)				
Range	1–64	45.8–75.6	2.60–2.97	4–190
Mean	19	65.5	2.72	46
CAI (n = 8)				
Range	0–9	69.3–74.3	2.61–2.72	20–140
Mean	3	73.0	2.64	48
SAC (n = 11)				
Range	7–54	49.5–68.5	2.68–3.00	3–1200
Mean	19	62.90	2.76	412
WCSB (n = 183)[a]				
Range	n/a	42.3–88.8	2.35–3.48	0–126 000
Mean	n/a	67.1	2.72	1415

Note: APT, Athabasca Polymetamorphic Terrane; CAI, Central Alberta Intrusions; SAC, Southern Alberta Craton; WCSB, Western Canada Sedimentary Basin.
[a]From Burwash, unpublished files.

Vulcan mantle low

The Vulcan mantle low (VML) is an arcuate northeast- to east-trending crustal feature, approximately 50 km wide and extending across most of southern Alberta (Fig. 8). Aeromagnetic and Bouguer gravity lows (Figs. 2, 3) closely follow the same trend. Using data from gravity surveys carried out in the 1950s and early 1960s, E.R. Kanasewich and, later, R.M. Clowes (Kanasewich 1968; Kanasewich et al. 1969; Clowes and Kanasewich 1972) carried out deep seismic reflection studies along a north–south profile, east of the town of Vulcan. Crustal thickness along this profile varied from 38 to 47 km, leading to the hypothesis of a "Southern Alberta Rift." The aeromagnetic low that parallels the rift was named the Vulcan low by Ross et al. (1991). Synthesis of potential-field, geochronologic, geochemical, and structural data have been used to suggest that the Vulcan structure is of a collisional nature (Hoffman 1988; Thomas et al. 1987; Ross et al. 1991; Hoffman 1990).

The depth-migrated reflection line 25 displays a prominent crustal thickening of 6 km (Figs. 7, 8) coincident with the gravity and magnetic signatures. The existence of the VML supports the concept of a collision of two blocks. Combining the original Lithoprobe time-migrated seismic profiles and potential-field modelling, Eaton et al. (1999) confirmed this interpretation. They suggest the Vulcan structure records crustal shortening produced by south-dipping subduction of the Loverna block (Hearne Province) beneath the Medicine Hat block (Wyoming Province), with the magnetic anomaly being produced by deep granitic intrusions and the flanking gravity highs by thrust-faulted, high-density crust.

Along line 25, depths to the Moho north of VML are uniform at 42 km. South of VML depths are variable from 44 to 47 km. This mantle topography has been explained by Lemieux et al. (2000) as due to imbrication of the Archean crust of the Medicine Hat block along southwest-dipping thrust faults. One of these faults has produced a "step" on the top of the mantle.

Conclusions

Over 1900 km of deep crustal reflection profiles were depth migrated to improve the resolution and obtain a more accurate model of crustal thickness variations along the profiles. A geologically reasonable velocity model, developed from velocity structures as determined for the Canadian craton using refraction methods and consistent with the inferences of rock velocity measurements, was employed. This model was updated on a trace-by-trace basis according to the local crustal thickness in an iterative fashion yielding uncertainties in the estimation of crustal depth of less than 2 km. Further, lateral variations in the velocities of the sedimentary column were incorporated. At present, the routines require substantial parallel computational resources.

The depth-migrated profiles (Fig. 7) show significant improvement over the unmigrated time sections. One measure of this quality is the good match between the depths to the top of the metamorphic basement predicted by the migration relative when compared to those known from drilling (within 100 m). However, a great deal of care must be taken to successfully carry out such migration on the long (18 s) records employed. In particular, residual deconvolution artefacts from the initial commercial processing and the substantially stronger amplitudes within the overlying sedimentary column complicated the process substantially.

The character of the Mohorovičić discontinuity varies over the extent of the profiles. The Moho appears as an isolated distinct reflection only in a small fraction of the profiles and is generally displayed as a sharp change in the reflectivity texture. At face value, the depth of such a change (ignoring the uncertainty introduced by the assumed velocity model) is better than 1 km. The loss of a clear change in character over adjacent lines acquired at slightly different times suggests that acquisition or processing differences can be important in producing data of sufficient quality for Moho observation. Moho depths were picked and a revised map of Moho depths produced, this shows a number of small wavelength (~50 km) features with thicknesses varying from a low of 36 km to a high of 48 km. These features include extensional crustal thinning in northwest Alberta here called the Spirit River mantle high, mantle faulting in excess of 10 km topography associated with the Snowbird tectonic zone, and the Vulcan structure in southern Alberta.

Depth migration is an expensive process, the present study required weeks of dedicated multiprocessor time. However, the process provides high quality images for structural interpretations. Most importantly, the images are directly in depth allowing for less ambiguous estimates of crustal thickness. Further, a number of subtle features such as the Spirit River mantle high described above are not as readily apparent in the time-migrated sections, especially after coherency filters have been applied. This alone provides a strong motivation to carry out depth migration on such profiles.

Acknowledgments

This paper is dedicated to the memory of Professor E.R. Kanasewich, a pioneer in deep crustal seismology. The authors wish to thank K. Vasudevan and R. Maier at the Lithoprobe Seismic Processing Facility, Calgary, Alberta, for their assistance and M. Burianyk for important insight in processing and especially with regards to refraction results. S. Phadke developed the parallel migration algorithm. Computer and Network Services personnel at the University of Alberta, Edmonton, Alberta, greatly assisted access to parallel computational facilities. Reviews by T. Boucher, F. Cook, J. Hall, and G. Ross are greatly appreciated. This work was supported by the National Science and Engineering Research Council of Canada grants to Drs. E.R. Kanasewich and D.R. Schmitt.

References

Agarwal, R.G. 1968. Regional correlation of geological and geophysical data in the Reindeer Lake area, northern Saskatchewan. Department of Mineral Resources, Province of Saskatchewan, Report 102.

Bickford, M.E., Van Schmus, W.R., MacDonald, R., Lewry, J.F., and Pearson, J.G. 1986. U–Pb geochronology project for the Trans-Hudson Orogen: Current sampling and recent results. *In* Summary of investigations, Saskatchewan Geological Survey, Miscellaneous. Report 86-4, pp. 101–107.

Braile, L.W., Hinze, W.J., von Frese, R.R.B., and Keller, G.R. 1989. Seismic properties of the crust and uppermost mantle of the coterminous United States and adjacent Canada. Geological Society of America Memoir, **172**: 655–680.

Bunks, C. 1992. Optimisation of the paraxial wave equation operator coefficients. *In* 62nd Annual International Meeting and Exposition, New Orleans, Louisiana. Society of Exploration Geophysicists, Expanded Abstracts, pp. 897–900.

Burianyk, M.J.A., Bouzidi Y., Phadke, S., and Kanasewich E.R. 1997. Seismic velocity models and depth migration imaging of the Alberta Basement. *In* Alberta Basement Transects Workshop. *Compiled by* G.M. Ross. Lithoprobe Secretariat, The University of British Columbia, Lithoprobe Report 59, pp. 9–22

Burwash, R.A., and Culbert, R.R. 1976. Multivariate geochemical and mineral patterns in the Precambrian basement of western Canada. Canadian Journal of Earth Sciences, **13**: 1–18.

Burwash, R.A., and Muehlenbachs, K. 1997. Tectonic setting of eastern Alberta basement granites inferred from Pearce trace element discrimination diagrams. *In* Alberta Basement Transects Workshop. *Edited by* G.M. Ross. Lithoprobe Secretariat, The University of British Columbia, Lithoprobe Report 59, pp. 35–49.

Burwash, R.A., Green, A.G., Jessop, A.M., and Kanasewich, E.R. 1993. Geophysical and petrological characteristics of the basement rocks of the Western Canada Basin. *In* Sedimentary Cover of the Craton in Canada. *Edited by* and J.D. Aitken and D.F. Stott. Geology of Canada, Vol. 5, pp. 55–77.

Burwash, R.A., Krupicka, J., and Wijbrans, J.R. 2000*a*. Metamorphic evolution of the Precambrian basement of Alberta. Canadian Mineralogist, **38**: 423–434.

Burwash, R.A., Chacko, T., Muehlenbachs, K., and Bouzidi, Y. 2000*b*. Oxygen isotope systematics of the Precambrian basement of western Canada: implications for Paleoproterozoic and Phanerozoic tectonics in northwestern Alberta. Canadian Journal of Earth Sciences, **37**: 1611–1628.

Carolan, J., and Collerson, K.D. 1988. The Virgin River shear zone in the Careen Lake area: field relationships and kinematic indicators. *In* Summary of investigations, 1988. Saskatchewan Geological Survey, Miscellaneous Report 88-4, pp. 92–96.

Chandra, N.N. 1966. Converted wave method for crustal structure. M.Sc. Thesis, University of Alberta, Edmonton, Alta.

Chandra, N.N., and Cumming, G.L. 1972. Seismic refraction studies in Western Canada. Canadian Journal of Earth Sciences, **9**: 1099–1109.

Christensen, N.I., and Mooney, W.D. 1995. Seismic velocity structure and composition of the continental crust: A global view. Journal of Geophysical Research, **100**: 9761–9788.

Claerbout, J.F. 1985. Imaging the Earth's Interior. Blackwell Scientific Publications, Boston, Mass.

Clowes, R.M., Kanasewich, E.R., and Cumming, G.L. 1968. Deep crustal seismic reflections at near-vertical incidence. Geophysics, **33**: 441–451.

Clowes, R.M., and Kanasewich, E.R. 1972. Digital filtering of deep crustal seismic reflections. Canadian Journal of Earth Sciences, **9**: 434–451.

Cook, F.A. 1995. Lithospheric processes and products in the southern Canadian Cordillera: A Lithoprobe perspective. Canadian Journal of Earth Sciences, **32**: 1803–1824.

Cumming, G.L., and Kanasewich, E.R. 1966. Crustal structure in Western Canada. Final Report Contract AF19 (628) 2835, Air Force Cambridge Research Laboratories (AFCRL), Bedford, Mass.

Davis, W.J., Berman, R., and Kjarsgaard, B. 1995. U–Pb geochronology and isotopic studies of crustal zenoliths from the Archean Medicine Hat block, northern Montana and southern Alberta: Paleoproterozoic reworking of Archean lower crust. *In* Alberta Basement Transects Workshop. *Edited by* G.M. Ross. Lithoprobe Secretariat, The University of British Columbia, Lithoprobe Report 47, pp. 329–334.

Dufresne, M.B., Eccles, D.R., McKinstry, B., Schmitt, D.R., Fenton, M.M., Pawlowicz, J.G., and Edwards, W.A.D. 1996. The Diamond Potential of Alberta, Alberta Geological Survey Bulletin, **63**.

Eaton, D.W. 1995. The Peace River Arch Industry Seismic Experiment (PRAISE-94): Summary of acquisition and processing procedures. *In* Alberta Basement Transects Workshop. *Edited by* G.M. Ross. Lithoprobe Secretariat, The University of British Columbia, Lithoprobe Report 47, pp. 1–8.

Eaton, D.W., and Ross, G.M. 1996. SALT and VauLT. *In* Alberta Basement Transects Workshop: summary of data acquisition and processing over the Vulcan low. *Compiled by* G.M. Ross., Lithoprobe Secretariat, The University of British Columbia, Lithoprobe Report 51, pp. 1–10.

Eaton, D.W., Ross, G.M., and Clowes, R.M. 1999. Seismic-reflection and potential-field studies of the Vulcan structure, Western Canada: A Paleoproterozoic Pyrénées? Journal of Geophysical Research, **104**: 23255–23270.

Ganley, D.C., and Cumming, G.L. 1974. A seismic reflection model of the crust near Edmonton, Alberta. Canadian Journal of Earth Sciences, **11**: 101–109.

Garland, G.D., and Burwash, R.A. 1959. Geophysical and petrologic study of the Precambrian of central Alberta, Canada. Bulletin of the American Association of Petroleum Geologists, **43**: 790–806.

Halchuk, S.C., and Mereu, R.F. 1990. A seismic investigation of the crust and Moho underlying the Peace River Arch, Canada. Tectonophysics, **185**: 1–19.

Hale, L.D., and Thompson, G.A. 1982. The seismic reflection character of the continental Mohorovičić discontinuity. Journal of Geophysical Research, **87**: 4625–4635.

Hammer, P.T.C., and Clowes, R.M. 1997. Moho reflectivity patterns—a comparison of Canadian LITHOPROBE transects. Tectonophysics, **269**: 179–198.

Hoffman, P.F. 1988. United plates of America, the birth of a craton: Early Proterozoic assembly, a growth of Laurentia. Annual Review of Earth and Planetary Science, **16**: 543–603.

Hoffman, P.F. 1990. Subdivision of the Churchill Province and extent of the Trans-Hudson Orogen. *In* The early Proterozoic Trans-Hudson Orogen of North America. *Edited by* J.F. Lewry and M.R. Stauffer. Geological Association of Canada (GAC), Special Paper 37, pp. 15–39.

Hyndman, R.D., and Lewis, T.J. 1995. Review: The thermal regime along the southern Canadian Cordillera Lithoprobe corridor. Canadian Journal of Earth Sciences, **32**: 1611–1617.

Kanasewich, E.R. 1966. Deep crustal structure under the plains and Rocky Mountains. Canadian Journal of Earth Sciences, **3**: 937–945.

Kanasewich, E.R. 1968. Precambrian rift: Genesis of stratabound ore deposits, Science, **161**: 1002–1005.

Kanasewich, E.R., and Cumming, G.L. 1965. Near-vertical-incidence seismic reflections form the "Conrad" discontinuity. Journal of Geophysical Research, **70**: 3441–3447.

Kanasewich, E.R., Clowes, R.M., and McCloughan, C.H. 1969. A buried Precambrian rift in western Canada. Tectonophysics, **8**: 513–527.

Kanasewich, E.R., Burianyk, M.J.A., Milkereit, B., White, D., and Ross, J.M. 1993. The Central Alberta Transect 1992 acquisition program: Preliminary results and progress report. *In* Alberta Basement Transects Workshop. *Edited by* G.M. Ross. Lithoprobe Secretariat, The University of British Columbia, Lithoprobe Report 31, pp. 1–8.

Kanasewich, E.R., Burianyk, M.J.A., Ellis, R.M., Clowes, R.M., White, D.J., Côté, T., Forsyth, D.A., Luetgert, J.H., and Spence, G.D. 1994. Crustal velocity structure of the Omineca belt, southeastern Canadian Cordillera. Journal of Geophysical Research, **99**: 2653–2670.

Kopp, C., Fruehn, J., Flueh, E.R., Reichert, C., Kukowski, N., Bialas, J., and Klaesvhen, D. 2000. Structure of the Makran subduction zone from wide-angle and reflection seismic data, Tectonophysics, **329**: 171–191.

Lemieux, S., Ross, G.M., and Cook, F.A. 2000. Crustal geometry and tectonic evolution of the Archean crystalline basement beneath the southern Alberta Plains, from new seismic reflection and potential-field studies. Canadian Journal of Earth Sciences **37**: 1473–1491.

Maureau, G.T.F.R. 1965. Crustal structure in Western Canada. M.Sc. thesis, University of Alberta, Edmonton, Alta.

McDonough, M.R., McNicoll, V. J., Schetselaar, E.M., and Grover, T.W. 2000. Geochronological and kinematic constraints on crustal shortening and escape in a two-sided oblique-slip collisional and magmatic orogen, Paleoproterozoic Taltson magmatic zone, northeastern Alberta. Canadian Journal of Earth Sciences **37**: 1549–1573

Meissner, R. (*Editor*). 1986. The Continental crust, a geophysical approach. International Geophysics Series, Academic Press, New York, 34.

Mereu, R.F., Majurndar, S.C., and White, R.E. 1977. The structure of the crust and upper mantle under the highest ranges of the Canadian Rockies from a seismic refraction survey. Canadian Journal of Earth Sciences, **14**: 196–208.

Mooney, W.D., and Meissner, R. 1992. Multi-genetic origin of crustal reflectivity: a review of seismic reflection profiling of the continental lower crust and Moho. *In* Developments in geotectonics. *Edited by* D.M. Fountain, R. Arculus, and R.W. Kay. Vol. 23, pp. 45–79.

Mooney, W.D., Laske, G., and Masters, T.G. 1998. CRUST 5.1: A global crustal model at 5° by 5°. Journal of Geophysical Research, **103**: 727–747.

Nataf, H.C., and Ricard, Y. 1996. 3SMAC: An a priori tomographic model of the upper mantle based on geophysical modelling. Physics of the Earth and Planetary Interiors, **95**: 101–122.

Nesbitt, B.E., and Muehlenbachs, K. 1995. Geochemical studies of the origins and effects of synorogenic crustal fluids in the southern Omineca belt, British Columbia, Canada. Geological Society of America Bulletin, **107**: 1033–1050.

Parrish, R.R. 1992. Eocene extensional faults: southern Cordillera Omineca Belt. *In* Geology of the Cordilleran Orogen in Canada. *Edited by* H. Gabrielse and C.J. Yorath. Geological Survey of Canada, Geology of Canada, No. 4 (Also Geological Society of America, The Geology of North America, Vol. G-2), pp. 660–663.

Richards, T.C., and Walker, D.J. 1959. Measurement of the thickness of the earth's crust in the Albertan Plains of western Canada. Geophysics, **24**: 262–284.

Ross, G.M., Parrish, R.R., Villeneuve, M.E., and Bowring, S.A. 1991. Geophysics and geochronology of the crystalline basement of the Alberta basin, western Canada. Canadian Journal of Earth Sciences, **28**: 512–522.

Ross, G.M., Milkereit, B., Eaton, D., White, D., Kanasewich, E.R., and Burianyk, M.J.A. 1995. Paleoproterozoic collisional orogen beneath the Western Canada Sedimentary Basin imaged by Lithoprobe crustal seismic-reflection data. Science, **23**: 195–199.

Ross, G.M., Eaton, D.W., Boerner, D.E., and Miles, W. 2000. Tectonics entrapment and its role in the evolution of continental lithosphere: An example from the Precambrian of western Canada. Tectonics, **19**: 116–134

Soller, D.R., Ray, R.D., and Brown, R.D. 1982. A new global crustal thickness map. Tectonics, **1**: 125–149.

Stephenson, R.A., Zelt, C.A., Ellis, R.M., Hajnal, Z., Morel-a-l'Huissier, P., Mereu, R.F., Northey, D.J., West, G.F., and Kanasewich, E.R. 1989. Crust and upper mantle structure and the origin of the Peace River Arch. Bulletin of Canadian Petroleum Geology, **37**: 224–235.

Tanimoto, T. 1995. Crustal structure of the earth. *In* Global Earth physics: a handbook of physical constants, AGU Reference Shelf. *Edited by* T.J. Ahrens. American Geological Union, Washington, D.C., Vol. 1, pp. 214–224

Thomas, M.D., Sharpton, V.L., and Grieve, R.A.R. 1987. Gravity patterns and Precambrian structure in the North American Central Plains. Geology, **15**: 489–492.

Tremblay, L.P. 1961. Geology, La Loche, Saskatchewan. Geological Survey of Canada, Map 10-1961, Scale 1 in to 4 mi (1 : 253 440).

Villeneuve, M.E., Ross, G.M., Theriault, R.J., Miles, W., Parrish, R.R., and Broome, J. 1993. Tectonic subdivision and U–Pb geochronology of the crystalline basement of the Alberta Basin, Western Canada. Geological Survey of Canada Bulletin, 447.

Walcott, R.I. 1968. The gravity field of the northern Saskatchewan and northeastern Alberta with maps. Department of Energy, Mines and Resources, Observatories Branch, Ottawa, Ont.

Walcott, R.I., and Boyd, J.B. 1971. The gravity field of northern Alberta, and part of Northwest Territories and Saskatchewan, with maps. Gravity map series, Earth Physics Branch, Department of Energy, Mines and Resources, Ottawa, Ont.

Wallis, R.H. 1970. A geological interpretation of gravity and magnetic data, northwestern Saskatchewan. Canadian Journal of Earth Sciences, **7**: 858–868.

Watanabe, R.Y. 1965. Petrology of cataclastic rocks of northeastern Alberta. Ph.D. thesis, University of Alberta, Edmonton, Alta.

Weaver, D.F. 1963. Seismological determination of crustal thickness in southern Alberta. M.Sc. thesis, University of Alberta, Edmonton, Alta.

Wright, G.N., McMechan, M.E., and Potter, D.E.G. 1994. Structure and architecture of the Western Canadian Sedimentary Basin. *In* Geological atlas of the Western Canadian Sedimentary Basin. *Compiled by* G. Mossop and I. Shetson. Canadian Society of Petroleum Geologists and the Alberta Research Council, Calgary, Alta., pp. 25–40.

Yilmaz, O. 1987. Seismic data processing. Investigations in Geophysics. Society of Exploration Geophysicists.

Zelt, C.A., and Ellis, R.M. 1989*a*. Comparison of near-coincident crustal refraction and extended vibroseis reflection data: Peace River Arch Region, Canada. Geophysical Research Letters, **8**: 843–846.

Zelt, C.A., and Ellis, R.M. 1989*b*. Seismic structure of the crust and upper mantle in the Peace River Arch region. Canada. Journal of Geophysical Research, **94**: 5729–5744.

Zhu, L. 2000. Crustal structure across the San Andreas Fault, Southern California, from teleseismic converted waves. Earth and Planetary Science Letters, **179**: 183–190.